Phenotypic analysis of catastrophic childhood epilepsy genes: The Epilepsy Zebrafish Project

Aliesha Griffin[1]*, Colleen Carpenter[1]*, Jing Liu[1], Rosalia Paterno[1], Brian Grone[1], Kyla Hamling[1], Maia Moog[1], Matthew T. Dinday[1], Francisco Figueroa[1], Mana Anvar[1, 2], Chinwendu Ononuju[2], Tony Qu[2], Scott C. Baraban[1, 2]

[1] Epilepsy Research Laboratory and Weill Institute for Neuroscience, Department of Neurological Surgery, University of California San Francisco, San Francisco, CA, 94143, USA

[2] Helen Wills Neuroscience Institute, University of California, Berkeley, CA 94720, USA

* These authors contributed equally to this work.

Correspondence should be addressed to scott.baraban@ucsf.edu

Abstract

Genetic engineering techniques have contributed to the now widespread use of zebrafish to investigate gene function, but zebrafish-based human disease studies, and particularly for neurological disorders, are limited. Here we used CRISPR-Cas9 to generate 40 single-gene mutant zebrafish lines representing catastrophic childhood epilepsies. We evaluated larval phenotypes using electrophysiological, behavioral, neuro-anatomical, survival and pharmacological assays. Phenotypes with unprovoked electrographic seizure activity (i.e., epilepsy) were identified in zebrafish lines for 8 genes; *ARX, EEF1A, GABRB3, GRIN1, PNPO, SCN1A, STRADA* and *STXBP1*. A unifying epilepsy classification scheme was developed based on local field potential recordings and blinded scoring from ~3300 larvae. We also created an open-source database containing sequencing information, survival curves, behavioral profiles and representative electrophysiology data. We offer all zebrafish lines as a resource to the neuroscience community and envision them as a starting point for further functional analysis and/or identification of new therapies.

Introduction

Catastrophic childhood epilepsies are characterized by intractable persistent seizures and are frequently associated with developmental delay, cognitive dysfunction and autism[1-3]. Many are rare genetic disorders lacking effective therapeutic options[4-6]. With technological advances and large-scale patient cohorts, genome-wide analyses have now identified *de novo* mutation in a single gene for most of these epilepsies[7-11]. These studies highlight the complexity of epilepsy, as mutations in genes coding for ion channels, ligand-gated receptors, solute transporters, metabolic enzymes, synaptic trafficking proteins, kinases, transcription factors, and adhesion molecules were identified. Unfortunately, our overall understanding of genetic epilepsies is severely limited as few experimental animal models exist, and human induced pluripotent stem cell derived two- or three-dimensional neuronal models fail to fully recapitulate the complex brain network seen in patients. Zebrafish, a small vertebrate with considerable genetic similarity to humans[12], offer an attractive alternative model to study these genetic mutations *in vivo*. Analysis of zebrafish mutants for human genes has provided valuable insight into complex circuits controlling behavior[13-17], evolutionarily conserved developmental programs[18-20] and drug candidates for a variety of diseases, including epilepsy[21-29].

Epilepsy classification, incorporating an understanding of different seizure types and comorbidities, is an essential clinical resource in evaluating patients and selection of anti-seizure treatments[30-33]. Clinical classification resources have evolved continuously since the 1960s. However, adaptation of this classification strategy to animal models[34], specifically zebrafish models developed for catastrophic epilepsies of childhood, is lacking. Because clinical seizure classifications promoted by the International League Against Epilepsy (ILAE)[33] are defined by the presence of unprovoked "self-sustained paroxysmal disorders of brain function", we focused our phenotyping effort on developing a standardized seizure classification scheme using electrophysiology data. Such a resource, broadly adapted, could be particularly useful for preclinical studies designed to characterize epilepsy phenotypes in any larval zebrafish model.

To better understand mechanisms underlying human genetic epilepsies, it is important to first identify clinically relevant phenotypes in an experimental model system[35]. Although efficient

gene inactivation in mice has contributed many pediatric epilepsy models[36-38], to generate dozens of mutant mouse lines followed by a systematic phenotypic analysis would require several decades of research. Using an efficient CRISPR-based gene editing strategy[39,40] we successfully generated 37 stable zebrafish lines representing human monogenic pediatric epilepsies. Large-scale phenotypic analysis of survival, behavior and electrographic brain activity was performed. We established read-outs to identify seizures at electrographic and behavioral levels, and an open-source online website to efficiently share data with the neuroscience community. As many of these zebrafish represent rare genetic diseases for which our understanding of pathophysiology remains largely unknown, they provide a rich resource to further investigate key etiological questions or utilization in high-throughput precision medicine-based therapy development.

Results

Generation of loss-of-function models for human epilepsy genes

We evaluated genes identified in a genome-wide association study from 264 patients with epileptic encephalopathies by the world-wide Epilepsy Genetics Initiative, Epi4K Consortium[8,41]. First, analysis of human genetic data was performed to identify genes where a loss-of-function (LOF) mutation was likely a causal mechanism of the epileptic phenotype. This limited our initial Epilepsy Zebrafish Project (EZP) choices to 63 gene candidates (Supplementary Table 1). Second, Epilepsy Genetics Initiative identified human genes were selected representing 57 orthologous zebrafish genes (Figure 1a). From this group, we identified 48 zebrafish genes that were high confidence orthologs (Figure 1b, homology scores; Supplementary Table 2) and examined expression data patterns with a primary focus on brain expression (Figure 1c). Third, RT-PCR confirmed gene expression for 46 zebrafish orthologs from the 4-cell to 7 dpf stage (Figure 1e) e.g., an early neurodevelopmental window wherein high-throughput studies would be feasible. To generate stable mutant lines, we used Cas9 with single *in vitro* transcribed guide RNA (with no predicted off-target sites) targeted towards the start of the protein coding sequence. A total of 46 zebrafish orthologous genes were targeted (Supplementary Table 3). This group includes a previously published *stxbp1b* mutant[42] and a novel *scn1lab* CRISPR mutant. Adult founders harboring predicted protein coding deletions

(Figure 1e; https://zebrafishproject.ucsf.edu) were confirmed and outcrossed for at least two generations. All EZP zebrafish were maintained as outcrossed lines with phenotypic assessment(s) performed on larvae generated from a heterozygous in-cross. For seven genes we could not obtain a viable line (*grin2aa*, *syngap1a*, *tbc1d24, prickl1a*, *plcb1*, *gosr2* and *stx1b*). In total, 37 novel EZP zebrafish lines were subjected to phenotypic screening described below.

Classification of seizure activity in larval zebrafish

We previously described minimally invasive local field potential recording (LFP) techniques to monitor brain activity in larval zebrafish[43] (Supplementary Figure 1). To identify epilepsy phenotypes in CRISPR-generated zebrafish lines, we obtained LFP recordings from 3255 larvae at 5 and 6 days post fertilization (dpf). We blindly recorded a minimum of 75 larvae per line, from at least three independent clutches. Larvae were randomly selected and genotyped *post hoc* to evaluate homozygote, heterozygote and wild-type (WT) phenotype-genotype correlations. Although long-duration, multi-spike large amplitude discharges are commonly described as seizure events in larval zebrafish models[23,44-47], a unified seizure classification system does not exist. As seizure classification is an essential clinical tool in identification of an epilepsy phenotype[48], we sought to establish the first classification scheme that could be universally applied to all zebrafish epilepsy models. An LFP electrophysiology-based scoring system covering all types of observed activity was established: (i) **Type 0**: the range of low voltage activities and patterns of small membrane fluctuations; (ii) **Type I**: low amplitude *interictal-like* sharp waveforms, with voltage deflections at least three times above baseline (duration range: 10 - 99 msec); and (iii) **Type II**: large amplitude *ictal-like* multi-spike waveforms, with voltage deflections at least five times above baseline (duration range: 45 - 5090 msec), often followed by a transient period of electrical suppression with no detectable events (Figure 2a). Based on this numeric classification, each 15 min recording epoch was assigned an LFP score by two independent investigators; cumulative averages can be seen in the heatmap for all 37 EZP-generated zebrafish lines (Figure 2b). We classified mutants with an average LFP score of 1.0 or above as an epilepsy phenotype. These included two genes previously determined to exhibit epilepsy phenotypes in zebrafish (e.g., *scn1lab*[23] and *stxbp1b* homozygotes[42]) and six novel zebrafish epilepsy lines (e.g., *arxa*, *eef1a2*, *gabrb3*, *pnpo, strada* homozygotes and *grin1b* heterozygotes). The percentage of EZP mutant larvae scored at Type II ranged from 29 to 83%

for epilepsy lines and a significant correlation between LFP classification scores versus percentage of Type II mutants was noted (Figure 2c; R^2 = 0.8790). Distribution of LFP classification scores for all WT larvae skewed toward Type 0 (mean WT score = 0.66; n = 781) and was significantly different than scoring distributions for mutant lines designated as epileptic (mean EZP-epilepsy score = 1.23; n = 190; Unpaired t-test $p < 0.0001$, t = 10.26, df = 969)(Figure 2d). The majority of LFP recordings from all lines were classified as Type 0 or 1 (79%; n = 3255; Figure 2e).

We next examined the frequencies, durations and spectral features of spontaneous epileptiform events recorded in all 8 EZP-epilepsy lines. To provide an unbiased quantitative analysis, Type I interictal- and Type II ictal-like electrical events were detected using custom software (see Methods; Figure 3) on homozygote and WT sibling larvae recordings. Representative LFP recordings (Figure 4b, top) with accompanying time-frequency spectrograms (Figure 4b, bottom) are shown for each EZP epilepsy line; individual LFP scoring distribution plots for mutants and WT siblings are shown at left. No difference in interictal-like (Type I) event frequency or duration was noted (Figure 4c). Ictal (Type II) events were more frequent and longer in duration for *scn1lab* mutant compared to WT; ictal event duration was shorter for *stxbp1b* mutants compared to WT (Figure 4d). Ictal event histograms showed similar overall distributions at a cumulative and individual level (Figure 5; Supplementary Figure 2). However, large-amplitude multi-spike ictal events when present in WT siblings were usually brief in duration, rarely exceeding 2.0 sec (Figures 5a, 5c) and less frequently encountered (Figures 5b, 5c) than those identified in EZP-epilepsy lines (also see cumulative distribution insets in Supplementary Figure 2a). Representative raw LFP traces and classification distribution plots for all 37 zebrafish lines can be explored on our open-source website, https://zebrafishproject.ucsf.edu, where users can also find information on homology, sequencing, survival and genotyping protocols.

EZP lines for understanding disease pathophysiology

Epileptic zebrafish can be used to study underlying neurobiological mechanisms, behavioral comorbidities and drug discovery. Many pediatric epilepsies are associated with increased mortality rates and thus, survival studies were performed on all EZP lines to evaluate larval health, confirm Mendelian genotyping ratios, and identify early death phenotypes (Figure 6a,

Supplementary Figure 3). Early fatality was noted in *aldh7a1*, *depdc5*, *scn8aa* and *strada* homozygous mutants that only survive between 8-10 dpf (Figure 6b).

We further performed a series of pilot experiments in all 8 EZP-epileptic lines to investigate other known pathophysiology. Epilepsy often manifests as convulsive behaviors in many of these genetic epilepsies. Prior work from our laboratory using chemically induced (Pentylenetetrazole ; PTZ) or an ENU-mutagenesis mutant for Dravet syndrome (*scn1lab*$^{s552/s552}$) describe a characteristic series of larval seizure-like behaviors, culminating in bursts of high-speed swim activity and whole-body convulsions[23,44]. Using these well-established models, we first developed a custom MATLAB algorithm to detect high-speed (≥ 28 mm/s), long-duration (≥ 1 s) behavioral events corresponding to these convulsive behaviors in freely behaving larvae (Figure 7). The MATLAB-detected behavioral event duration was similar to that measured for Type II ictal-like events in LFP recordings (see Figure 5). As expected, the EZP generated *scn1lab* mutant larvae displayed significantly higher velocity movements and higher frequencies of convulsive-like events compared to WT sibling controls; similar results were obtained with *scn1lab*$^{s552/s552}$ larvae. There was no difference in the total distance traveled between WT and homozygous mutants in these lines (Figure 6c). Maximum velocity and total distance measurements show that *arxa* larvae are hypoactive and they had no detectable high-speed, long-duration events during these 15 min recording epochs (Figure 6c; Figure 6d, representative traces). We observed that the duration of high speed events in *scn1lab*$^{s552/s552}$ larvae were significantly longer than in WT sibling controls (Figure 6e). No significant behavioral phenotypes were seen in the other epileptic lines (Supplementary Figure 4).

ARX-related epilepsies are categorized as "interneuronopathies"[49] and *Arx* mutant mice exhibit a reduced number of interneurons in both neocortex and hippocampus[50,51]. Using volumetric light-sheet microscopy imaging in larval *arxa* mutants co-expressing a green fluorescent protein (GFP) in *Dlx*-labeled interneurons[52], we confirmed a significant reduction in interneuron density for homozygous *arxa* mutant larvae compared to WT sibling controls (Figure 8a). *EEF1A2* mutations are associated with neurodevelopmental deficits in some patients.[53] Using conventional morphological analyses measuring overall head length, midbrain/forebrain width

and body length on *in vivo* images from *eefla2* mutant larvae and WT siblings at 5 dpf, we noted no differences (Figure 8b).

Patients with *GABRB3* mutations, like many of the genes studied here, are often classified as pharmaco-resistant[54]. Using a 1 hr LFP recording protocol, we evaluated electrographic seizure activity in *gabrb3* mutants treated with standard antiepileptic drugs (AEDs): carbamazepine, valproate and topiramate. In these zebrafish mutants, carbamazepine suppressed high-frequency interictal-like and long duration multi-spike ictal-like epileptiform discharges (Figure 8c). Patients with *ALDH7A1* mutations are associated with pyridoxine-dependent encephalopathy. Using a CRISPR-generated *aldh7a1*^{ot100} mutant, Pena et al. reported hyperactive behavior and spontaneous electrographic seizures in fed larvae starting at 10 dpf; 10 mM pyridoxine treatment rescued these phenotypes[46]. The unperturbed EZP generated *aldh7a1* mutant larvae die prematurely between 7 and 9 dpf. Daily 10 mM pyridoxine effectively extended the median survival of *aldh7a1* mutant larvae to that observed in heterozygote and WT sibling controls (Figure 8d).

Discussion

Progress in exploring pathogenesis, and developing new therapies, for monogenic epilepsies is complicated by limited availability of preclinical animal models for many of these genes. The emergence of zebrafish as a vertebrate model system amenable to genetic manipulation holds much promise toward accelerating progress in understanding these rare epilepsies. Here we utilized CRISPR/Cas9 and a battery of larval zebrafish assays to systematically evaluate 40 different single gene mutations identified in this population. We determined that homozygous deletion of *arxa*, *eef1a2*, *gabrb3*, *pnpo*, *scn1lab*, *strada* and *stxbp1b* or heterozygous loss of *grin1b* result in recurrent unprovoked electrographic seizures (i.e., epilepsy). In addition, we developed an electrophysiology-based classification system that can be used to identify seizures in any larval zebrafish model. Finally, we show that clinically relevant phenotypes such as interneuron loss (*arxa*) or pharmaco-resistance (*gabrb3*) can be recapitulated in zebrafish models.

Although, CRISPR/Cas9 works with remarkable efficiency to disrupt gene function in zebrafish[39,40], recent large-scale efforts have not reported on epilepsy or clinically-relevant functional outcome measures[16,17] . To present robust and well-controlled functional assays, we outcrossed all EZP lines a minimum of three generations and blindly analyzed homozygous, heterozygous and WT siblings. This approach avoids off-target or toxicity effects from microinjection or CRISPR/Cas9 editing that might cause identification of false positives. A limitation typical of these types of CRISPR-based larval zebrafish studies, focused primarily on novel genes, is that the full spectrum of tools (antibodies, etc.) or functional assays (single-cell electrophysiology) necessary to confirm LOF mutation are not available. Nonetheless, epileptic activities seen in CRISPR/Cas9 deficient (*aldh7a1*)[46,55] or ENU-generated (*scn1lab*$^{s552/s552}$)[23] zebrafish were successfully recapitulated here. Interestingly, but perhaps not surprisingly, the majority of our CRISPR-generated single gene LOF zebrafish mutants were not associated with epilepsy phenotypes at this stage of larval development (5-6 dpf). It is possible that many of these single gene mutations are one factor in the emergence of epilepsy in humans, but full clinical phenotypes rely upon polygenic factors[56,57], epigenetics[53] or environmental issues such as early-life febrile seizures[58]. Developmental considerations are an additional confounding factor[2,3], as clear epileptic phenotypes may emerge at later juvenile or adult timepoints. Although a potential limitation for interpretation of these studies, we chose to focus this initial phenotypic screening effort on larval developmental ages that would lend themselves to future high-throughput drug discovery. Where single gene mutant mice are available for electrophysiology comparisons a similar lack of unprovoked seizure phenotypes have been reported e.g., *Cdkl5*[59,60], *Chd2*[61] or *Depdc5*[62]. Further, the frequency and severity of seizure activity in patients with single gene mutations can also be variable e.g., *SCN8*[63], *PCDH19*[64], *MEF2C*[65], *CDKL5* and *ARX*[66], which highlights the complexity of modelling rare epilepsy gene candidates.

Our previous studies established the presence of hyperactive and seizure-like (stage III) behaviors in PTZ-treated WT larvae and spontaneously in *scn1lab*$^{s552/s552}$ mutant larvae, a model of Dravet syndrome[23,44]. These stage III behaviors are defined as brief clonus-like convulsions followed by a loss of posture, where a larvae falls on its side and remains immobile for 1–3 s (manually scored)[44]. Behavioral readouts were instrumental in primary screens aimed at finding novel anti-epileptic drugs that treat Dravet syndrome, ultimately allowing us to test over 3500

drugs in less than 5 years[23,24,27] and advancing our lead candidate to clinical trials (https://clinicaltrials.gov/ct2/show/NCT04462770). Here, we further refine our definition of seizure-like movements as events ≥ 28 mm/s in velocity and ≥1 s in duration and created a MATLAB algorithm to efficiently detect these events in our behavioral assays; total distance moved was not a reliable measure of these events. Interestingly, of our 8 EZP-epilepsy CRISPR lines, only the most robust phenotypic line (*scn1lab* mutants) had significantly more seizure-like behavioral events compared to controls, suggesting that hyper-locomotion alone may not be sufficient to identify epileptic phenotypes. Interestingly, hypo-locomotion seen here in *arxa* mutant larvae [also reported in *tsc2*[67] and *gabrg2*[68] mutants, respectively] may represent a pathological behavioral state. Ultimately and mimicking clinical diagnoses of epilepsies using video-electroencephalographic monitoring[2,30,44], our electrophysiology-based screening approach successfully identified epileptic activity that was not easily detected in locomotion-based assays. Although simple locomotor readouts have grown popular as seizure assays[69-74], this study emphasizes the rigor necessary to accurately identify epileptic phenotypes in zebrafish and suggests that sole reliance on behavior may lead to misleading conclusions during phenotyping and/or drug discovery efforts.

Overall, the Epilepsy Zebrafish Project demonstrates the power of large-scale phenotype-based analyses of human gene mutations and all mutant lines are available to the scientific community (https://zebrafishproject.ucsf.edu). These CRISPR-generated zebrafish models have two important advantages: first, they provide a valuable *in vivo* model system to explore underlying pathophysiological mechanisms in rare genetic epilepsies. Second, they provide an easily accessible preclinical model system for high-throughput drug discovery and therapy development that is far more efficient than rodent models. Pilot neurodevelopmental and pharmacological data was provided for several epileptic zebrafish lines here as a potential starting point for further investigations. We anticipate, and hope, that future studies using these zebrafish will help us to better understand genetic disorders and further the ultimate vision of precision medicine.

Figure Legends

Figure 1| The Epilepsy Zebrafish Project (EZP). (**a**) Overview of the zebrafish epilepsy disease model discovery workflow from human genome wide association studies (GWAS) to generation of zebrafish models and phenotypic characterization. (**b**) Tissue expression profiles of EZP zebrafish target genes. Heatmap represents the maximum number of sequence reads for each gene per tissue. (**c**) Developmental gene expression profiles for EZP lines. (**d**) Representative frame-shift mutant lines confirmed for *depdc5* and *eef1a2*.

Figure 2| Seizure classification using electrophysiological recording identifies epileptic zebrafish lines. (**a**) LFP recordings representing Type 0 (low voltage, small or no membrane fluctuations), Type I (low amplitude, sharp *interictal-like* waveforms) and Type II (low frequency, sharp *ictal-like* waveforms with large-amplitude multi-spike events and post-ictal slowing) scoring activity. For each example a color-coded event rate histogram (top), full 15 min LFP recording (middle), and high-resolution LFP close-up (red box, red trace at bottom) are shown. (**b**) Heatmap showing mean larval zebrafish LFP recording scores for all 37 EZP zebrafish lines ranked from highest homozygote score to lowest; N = 77 to 127 larvae per gene (see https://zebrafishproject.ucsf.edu for N values on each individual line). A threshold of a mean LFP score > 1.0 was classified as a an EZP line exhibiting epilepsy (indicated in bold font: *scn1lab*, *arxa*, *strada*, *stxbp1b*, *pnpo*, *gabrb3*, *eef1a2* and *grin1b*). (**c**) Regression plot for all 37 mutants showing mean LFP score versus % of Type II larvae for each homozygote. 7 homozygote and 1 heterozygote lines highlighted in "EZP-epi" box as clearly differentiated from cluster of 31 non-epileptic EZP lines with LFP scores < 1.0. Simple linear regression R^2 = 0.8790; ***Significant deviation from zero, $p < 0.0001$; DFn, DFd = 1, 36. (**d**) Violin plots of all LFP scores recorded for EZP-epilepsy lines (N = 190) compared to all WT control siblings (N = 783). Note: Type 2 epileptiform events were only observed in 14.7% of all WT larvae. (**e**) Distribution of Type 0, I and II scores for all WT, heterozygote and homozygote larvae screened by LFP recordings (N = 3255).

Figure 3| Automated interictal-like event quantification (**a**) A representative LFP recording with interictal-like events. A voltage threshold (0.15 – 0.25 mV, depending on the noise level) was set for event detection. Data was binarized by threshold: super-threshold data points were scored as 1, and under-threshold data points were scored as 0. (**b**) A data binning method was

used for automated quantification of interictal-like events: 0.01 sec binning in 0.5 sec time window. In each window, value of the first bin was calculated, which is the ratio of active data points to the number of total data points within the window. (**c**) Color raster plots were created according to the raster score. A raster score threshold (0.2 – 0.4) was set to define the start and end of an event. (**d**) Comparison between interictal-like event durations measured automatically and manually. A 10 sec representative epoch from each recording will be used as a testing sample to optimize the algorithm. Voltage and raster score thresholds were chosen when the difference between automated and manual results is less than 3% of manual measurements.

Figure 4| Electrographic seizure activity in epileptic zebrafish mutant lines. (**a**) Schematic of recording configuration and protocol for electrophysiology-based screening of larval zebrafish. (**b**) Representative raw LFP recording traces (top, right) along with a corresponding wavelet time-frequency spectrogram (bottom, right) and LFP scoring distribution plot for WT and mutant larvae (left) are shown for each EZP-epilepsy line. Type 0, I and II scoring as in Figure 2. A representative WT LFP recording with the corresponding wavelet time-frequency spectrogram is shown in Supplementary Figure 5. Scale bar = 500 μV. Representative LFP recordings and distribution plots for all 37 lines can be found online (https://zebrafishproject.ucsf.edu). (**c**) Cumulative plots of interictal event frequency (left) and duration (right) for all EZP-epilepsy lines compared to WT sibling controls. Each point represents mean of all interictal events in a single 15 min larval LFP recording detected using custom software in MATLAB (N = 9775, WT; N = 6750, *scn1lab*; N = 2550, *arxa*; N = 5790, *strada*; N = 6750, *stxbp1b*; N = 3538, *pnpo*; N = 3455, *gabrb3*; N = 4335, *eef1a2*; N = 6610, *grin1b**). (**d**) Cumulative plots of ictal event frequency (left) and duration (right). Each point represents all ictal events in a single 15 min larval LFP recording detected using custom software in MATLAB (N = 56, WT; N = 62, *scn1lab*; N = 26, *arxa*; N = 26, *strada*; N = 48, *stxbp1b*; N = 22, *pnpo*; N = 59, *gabrb3*; N = 27, *eef1a2*; N = 55, *grin1b**). *for *grin1b* designates heterozygote. ***$p < 0.01$, ANOVA with Dunnett's multiple comparisons test.

Figure 5| Distribution of ictal events. Histograms depict number and duration of ictal events measured using a custom MATLAB-based program for (**a**) all sibling wild-type (WT) larvae

from EZP epilepsy lines and (**b**) same for epileptic zebrafish lines (EZP)-Epi. Box-and-whisker plots showing the distribution of ictal event durations; mean and minimum/maximum values are shown (*insets*). (**c**) Estimation plot showing that ictal event duration for WT (1.134 ± 0.075 sec; N = 56) is shorter than for Epi-EZP (1.353 ± 0.043 sec; N = 299); Non-parametic t-test $*p$ = 0.0352, t = 2.115, df = 353). Each dot on the top plot represents the duration (measured in msec) for one individual ictal event.; each dot in the bottom plot represents ictal event frequency for one LFP recording. LFP recording epochs were 15 min.

Figure 6| Survival and behavioral phenotypes. (**a**) Heatmap displaying median wild-type (WT), heterozygote (HET) and homozygote mutant (MUT) larval survival for EZP lines. Range extends from 8 dpf (red) to 13 dpf (blue). Asterisks indicate MUTs with significant survival deficits compared WT control siblings; $p < 0.05$, log rank test. (**b**) Lines with significant survival deficits. (**c**) Quantification of the basal locomotor activity of epileptic lines after 1 hr habituation in DanioVision chamber. Maximum velocity and total distance traveled were extracted directly from EthoVision XT 11.5 software while the number of events ≥ 28 mm/s, termed high speed events (HSE), and long duration HSE (≥ 1 s) were scored using a MATLAB algorithm (*scn1lab*^{552} WT N = 19, MUT N = 31; *scn1lab* WT N = 21, MUT N = 16; *arxa* WT N = 25, MUT N = 22; *strada* WT N = 27, MUT N = 31; *stxbp1b* WT N = 26, MUT N = 43; *pnpo* WT N = 42, MUT N=40; *gabrb3* WT N = 35, MUT N = 36; *eef1a2* WT N = 30, MUT N = 27 and *grin1b* WT N=29 and HET=57). (**d)** Representative traces of *arxa* WT and MUT movement. (**d**) Comparison of duration of HSE in *scn1lab* ENU and CRISPR larvae. Displayed as mean ± SEM, One-Way ANOVA was used to determine the significance of both HET and MUT behavior for all lines (See Supplementary Figure 4 for expanded data set). *Post hoc* Dunnett multiple comparison test, $*p \leq 0.05$, $**p \leq 0.005$, $**p < 0.0001$.

Figure 7| Automated detection of behavioral seizure-like events. (**a**) Example of low-speed movement in a WT larva (left - green), high-speed movement in the same WT larva (middle - orange), and seizure-like movement in a PTZ-treated larva (right - red). Top traces represent the larvae track during 15 min recording in a 96-well plate. The bottom panels show speed values across time for the events highlighted. Note the short and long duration in the high-speed events in WT and PTZ-treated larvae, respectively. (**b**). Distribution of maximum speed (left) and

duration (right) across all movements in WT larvae (n: 109) during the 15-minute recording session. The average maximum speed was 10.5 mm/sec and the duration of the events was less than 1 second. (**c**). Frequency of seizure-like movements (defined as events with maximum speed greater than 28 mm/sec and duration greater than 1 second) in control and PTZ-treated larvae at different concentrations after 10, 30 and 60 minutes (two-way ANOVA $p<0.05$). Note the increased number of events with increasing PTZ dose and the lower number when using 15 mM after 60 minutes due to increased larvae mortality.

Figure 8| Developmental and pharmacological characterization. (**a**) Representative images of *dlx*-GFP expressing interneurons in *arxa* MUT larvae (N = 8) and WT siblings (N = 12) obtained from volumetric light sheet imaging microscopy. Unpaired two-tailed t-test $*p = 0.0268$; t = 2.411, df = 18) (**b**) High resolution images of larvae were taken using a SteREO Discovery.V8 microscope (Zeiss) and overall head length, midbrain width, forebrain width and body length were quantified in *eef1a2* MUT (N=6) and WT (N=5) larvae. (**c**) Representative 1 hr LFP traces from *gabrb3* MUT larvae exposed to AEDs. The first ~10 min of the recording (in red) represents baseline. Drugs were bath applied at a concentration of 0.5 mM; N = 3-6 fish per drug. Results from carbamazepine treatment shown as violin plot. Unpaired two-tailed t-test $**p < 0.0001$; t = 6.344, df = 10). (**d**) Kaplan-Meier survival curves for *aldh7a1* WT, *aldh7a1* HET and *aldh7a1* MUT larvae treatment with 10 mM pyrodixine (pyr) or vehicle for 30 mins daily starting at 4 dpf. Median survival for vehicle treated *aldh7a1* WT = 12 dpf (N = 12), *aldh7a1* HET = 11.5 dpf (N = 22) and *aldh7a1* MUT = 8 dpf (N = 9). Median survival for 10 mM pyridoxine (pyr) treated larvae for *aldh7a1* WT = 12 dpf (N = 21), *aldh7a1* HET = 12 dpf (N = 34) and *aldh7a1* MUT = 12 dpf (N = 13).

Supplementary Figure 1| Local field potential recordings are minimally invasive. (**a**) Five dpf larvae were left freely swimming in embryo medium or subjected to agar embedding or agar embedding with electrode implantation, and behavior was tracked 4 hr and 24 hr after each treatment. Results show no significant differences in the total distance traveled (**b**) or maximum velocity (data not shown) of larvae when compared across the treatment groups. Data displayed as mean ± SEM.

Supplementary Figure 2| Distribution of ictal events. Histograms depict number and duration of ictal events cumulatively (**a-b**) and across individual EZP-epilepsy lines (**c-j**). Asterisk for *grin1b* designates heterozygote. Interictal events were measured using a custom MATLAB-based program for EZP-epilepsy lines and WT siblings.

Supplementary Figure 3| Kaplan-Meier survival curves for zebrafish CRISPR lines. Plots of survival for unfed WT, heterozygous and homozygous larvae across all zebrafish lines.

Supplementary Figure 4| Basal locomotor activity of epileptic zebrafish lines. Five dpf larval zebrafish were tracked in the behavioral assay and graphs depict (**a**) total distance traveled, (**b)** maximum velocity, (**c**) number of high-speed events (HSE) and (**d**) number of long duration HSE observed across the various lines. Total distance and maximum velocity were extracted directly from EthoVision XT 11.5 software while the number of events ≥ 28 mm/s (HSE) and long duration HSE (≥1 s) were scored using an in-house MATLAB algorithm. Data displayed as scatter plots showing individual larval values and error bars represent mean and SEM. Statistics calculated using One-way ANOVA and *post hoc* Dunnett multiple comparison test, $*p \leq 0.05$, $**p \leq 0.005$, $**p < 0.0001$.

Supplementary Figure 5| Wild-type recording. Representative raw LFP recording trace (top) along with a corresponding wavelet time-frequency spectrogram (bottom) for a representative WT zebrafish larvae. Scale bar = 500 μV.

Methods

Zebrafish Husbandry

All procedures described herein were performed in accordance with the Guide for the Care and Use of Animals (ebrary Inc., 2011) and adhered to guidelines approved by the University of California, San Francisco Institution Animal Care and Use Committee (IACUC approval *#:* AN171512-03A). The zebrafish lines were maintained in a temperature-controlled facility on a 14:10 hour light:dark cycle (9:00 AM -11:00 PM PST). Juvenile and adult zebrafish were housed on aquatic units with an automated feedback control unit that maintained the system water

conditions within the following ranges: temperature; 28-30 °C, pH; 7.5-8.0 and conductivity; 690-740 mS/cm. Juveniles (30-60 dpf) were fed twice daily, once with JBL powder (JBL NovoTom Artemia) and the other with JBL powder + live brine shrimp (Argent Aquaculture). Older juveniles and adults were also fed two times per day, first with flake food (tropical flakes, Tetramin) and then with flake food and live brine shrimp. Zebrafish embryos and larvae were raised in an incubator kept at 28.5 °C under the same light-dark cycle as the facility. The solution or 'embryo medium' used for the embryos and larvae consisted of 0.03% Instant Ocean (Aquarium Systems, Inc.) and 0.000002% methylene blue in reverse osmosis-distilled water. Larvae were fed with powder (6-10 dpf) or JBL powder + brine shrimp (11-29 dpf).

Zebrafish homology prediction

To improve our confidence in modeling epilepsy at the genetic level in zebrafish, we established a zebrafish homology score. To determine the homology score the percent protein identity and DIOPT score was used. The percent protein identity was established from Ensembl (GRCz10) using the predicted human orthologue gene. When the human orthologue gene was not predicted by Ensembl, a Clustal Omega analysis was performed using standard parameters. The DIOPT score was established using the MARRVEL (http://marrvel.org/) database and is the number of orthologue prediction tools that predicted a given orthologue pair. Twelve orthologue prediction tools (Comara, Eggnog, Homologene, Inparanoid, OMA, OrthoDB, orthoMCL, Panther, Phylome, RoundUP, TreeFam and ZFIN) were used to predict zebrafish orthologs. The homology score represents the average of the percent identity and the DICOT score as a percentage. A gene with a homology score >65 was considered for the EZP.

Zebrafish gene expression analysis

Adult tissue expression was determined using the Phylofish database[75]. Development expression was determined using semi-quantitative RT-PCR. Pools of 25 to 50 zebrafish embryos or larvae were collected at 4-cell, 32-cell, high, sphere, 12 hpf, 1, 2, 3, 4, 5, and 7 dpf for expression analysis. Total mRNA was extracted from whole embryos or larvae using a phenol/chloroform extraction protocol. After extraction, 1 µg of purified RNA was treated with DNaseI and retrotranscribed to cDNA using following SuperScript IV Reverse Transcriptase (8091050, Invitrogen) the manufacturer's protocol. The temporal expression of genes was characterized RT-

PCR using GoTaq Master Mix (M712C, Promega) and oligonucleotide sequences are listed at https://zebrafishproject.ucsf.edu. Thermal cycling conditions included an initial denaturation at 95°C for 5 min, followed by 40 cycles at 95°C for 30 sec, 56°C for 30 sec, and 72°C for 30 sec and a final incubation at 72°C for 7 min.

Generation of CRISPR mutant lines

Zebrafish mutant lines of the 40 genes were generated using CRISPR-Cas gene editing in Tupfel Long-Fin (TL) wild-type zebrafish (ZIRC). CRISPRScan was used to identify sgRNA sequences with high predicted cut efficiencies for early exons and sgRNAs were synthesized using T7 in vitro transcription with the MEGAshortscriptTM T7 Transcription Kit (AM1354, ThermoFisher). To minimize off target-effects, we selected target sites with the lowest number of potential mutagenesis and with a minimum of three mismatches with every other site in the genome. Fertilized embryos (1-2 cell stage) were co-injected with ~2 nl of sequence-specific sgRNA (~10-25 ng/µl), Cas9 mRNA (~250 ng/µl) and 0.4% rhodamine b. At 1 dpf, embryos were sorted for fluorescence and genomic DNA extracted using Zebrafish Quick Genotyping DNA Preparation Kit (GT02-02, Bioland Scientific) from pools of 5-10 healthy, microinjected and un-injected larvae. The samples were Sanger sequenced to assess gene editing at the guide target site. Once editing was confirmed, the remaining embryos were raised to adulthood. Resulting F0 mosaic adults, confirmed by Sanger sequencing DNA from fin-clips, were crossed with TL zebrafish to create stable heterozygote F2 and greater generations of breeders for our experiments. Guide RNA, primer sequences and PCR protocols for all lines can be found in Supplementary Table 3. All experiments were done blinded using unfed larvae between 3-14 dpf. At this stage larvae are sexually indistinguishable.

Electrophysiology

Zebrafish larvae (5-6 dpf) were randomly selected, briefly exposed to cold anesthesia or pancuronium (300 µM) and immobilized, dorsal side up, in 2% low-melting point agarose (BP1360-100, Fisher Scientific) within a vertical slice perfusion chamber (Siskiyou Corporation, #PC-V). Slice chambers containing one or two larvae, were placed on the stage of an upright microscope (Olympus BX-51W) and monitored continuously using a Zeiss Axiocam digital camera. Under visual guidance, gap-free local field potential recordings (LFP; 15 min duration)

were obtained from optic tectum using a single glass microelectrode (*WPI glass #TW150 F-3*); ~ 1 μm tip diameter; 2 mM NaCl internal solution), as described[43,44]. LFP voltage signals were low-pass filtered at 1 kHz (-3 dB; eight-pole Bessel), digitized at 10 kHz using a Digidata 1320 A/D interface (Molecular Devices) and stored on a PC computer running AxoScope 10.3 software (Molecular Devices). For pharmacology experiments, continuous gap-free LFP recordings were made for 1 hr and drug concentrations are based on previously published data[23,44]. Larvae were gently freed from agarose at the conclusion of recording epochs for *post hoc* genotyping by investigators blind to status of the experiment. Electrophysiology files were also coded for *post hoc* analysis off-line. Experiments were performed on at least three independent clutches of larvae for each line; a minimum of 75 larvae were screened per line. Individual abnormal electrographic seizure-like events were defined as: (i) brief interictal-like events comprised of spike upward or downward membrane deflections greater than 3x baseline noise level or (ii) long duration, large amplitude ictal-like multi or poly-spike events greater than 5x baseline noise level. Quantification of epileptiform events was performed using Clampfit 10.3 (Molecular Devices) or custom MATLAB (MathWorks; Figure 3) software by investigators blind to status of the experiment. A binning method combined with a sliding window algorithm was used to calculate the active level of the signal within the current time window. The value of each bin was used to identify the start and end of an event. We used a range of voltage thresholds (0.15 – 0.25 mV, depending on the noise level) and a relative threshold (3x Standard Deviation) for detection of interictal events. By comparing manual-auto counting results of a testing data sample for each recording (Figure 4d), we fine-tuned the threshold detection for each recording to a level where auto counting results were close to the manual counting results (< 3% difference). All files were un-coded and combined with genotyping data at the end of this process.

Larval Behavior

Basal locomotion

Behavioral studies conducted on select EZP lines utilized a 96-well format and automated locomotion detection using a DanioVision system running EthoVision XT 11.5 software (DanioVision, Noldus Information Technology). Zebrafish larvae were transferred from their home incubator to the test room at least 10 min before the experiment. After larvae were

individually transferred to wells in ~150 µl of embryo media, the 96 well-plate was placed in the DanioVision observation chamber and left undisturbed for 1 hr. Larval movement was tracked for 15 min at 25 frames per sec with the following detection settings: method; DanioVision, sensitivity; 110, video pixel smoothing; low, track noise reduction; on, subject contour; 1 pixel (contour dilation, erode first then dilate), subject size; 4-4065. For each zebrafish line, experiments were performed with at least 3 different clutches and *post hoc* genotyping. Mean and maximum velocity of each larvae were calculated. Additionally, high-speed seizure behaviors were scored using a MATLAB algorithm developed by our laboratory and validated on PTZ and *scn1lab* seizure models (Figure 7).

Seizure-like behavioral event classification

To classify larval movements, we first processed the videos with EthoVision software 11.5 (Noldus) to identify a larva's position at an acquisition rate of 25 frames/sec, using the same detection settings listed in the 'basal locomotion' assay, except with the track noise reduction off. Using custom-written MATLAB-based software, we then extracted movement events defined as times when larvae speed exceeded a threshold of 0.9 mm/sec for at least 160 msec. Adjacent events were combined if the time interval was less than 40 msec. Furthermore, when the maximum speed within an event was lower or higher than a cutoff threshold, the movement events were classified into low- and high- speed events, respectively. For the analysis in Figure 7, we calculated the distribution of all movements in a large control group of larvae and then identified the speed value threshold at 1.5x Standard Deviation to be used as a cutoff threshold, unless otherwise specified. Similar results for larval WT movement speeds and duration have been previously reported[76]. Seizure-like events were defined as high-speed movement events that lasted longer than 1 sec validated on PTZ and *scn1lab* seizure models.

Behavioral effects of electrode implantation

WT larvae (5 dpf) in 100 mm petri dishes were transferred to the test room and subjected to one of three treatments:

<u>Treatment 1</u>: Larvae were briefly anesthetized in pancuronium (300 µM) and then immobilized in 2% agarose dorsal side up on a recording chamber. About 3 ml of recording media was added

to the chamber then a glass micro-electrode was positioned in the forebrain for LFP recording as previously described[43,44]. After 15-30 min, the electrode was removed and the larva gently released from agarose and transferred to a petri dish with embryo medium.

Treatment 2: Larvae were briefly anesthetized in pancuronium (300 µM) and then immobilized in 2% agarose dorsal side up on a recording chamber. After 15-30 min, the larvae were gently released from the agarose and transferred to a petri dish with embryo medium.

Treatment 3: Larvae were left undisturbed in original petri dish.

At the end of the experiment, all treatment groups were returned to the home incubator until behavioral experiments. Four hours after treatment, larvae were returned to test room and left undisturbed for 10 min. Larvae were individually transferred to a 96 well plate in ~150 µl of embryo media and the plate then placed in the DanioVision observation chamber. After 15 min, larval movement was tracked for 30 min using settings outlined in 'basal locomotion'. Once completed, the plate was removed and returned to the home incubator. The same steps were followed to record behavior 24 hr post-treatment.

Survival Assay

For each line, 20-24 zebrafish larvae were randomly selected from at least two clutches and were placed in a 100 mm petri dish containing ~40 ml egg water. The larvae were monitored twice daily and dead larvae were lysed using Bioland Zebrafish Quick Lysis Kit. Larvae were not fed throughout the duration of the assay. This was done to eliminate potential effects of variations in larval feeding, ultimately providing us with a robust method to identify early-stage larval lethality phenotypes. Unfed larvae typically die by 12 dpf[77]. Samples were genotyped using protocols specified in Supplementary Table 3.

Pyridoxine supplementation: aldh7a1 survival

At 4 dpf, larvae were placed individually in 24 well plate with 500 µl 10 mM pyrodixine or egg water (control). Treatment was removed and replaced with fresh egg water. Larvae were then treated with 500 µl 10 mM pyrodixine or egg water (control) for 30 min daily. During daily

monitoring, dead larvae were lysed using Bioland Zebrafish Quick Lysis Kit. Samples were genotyped using protocols specified in Supplementary Table 3.

Imaging

For morphology measurements in the *eef1a2* CRISPR line, larvae were placed individually in one well of a μ-well microscope slide (iBidi) and high-resolution images obtained using an optiMOS CMOS camera (QImaging) camera mounted on a SteREO Discovery.V8 stereomicroscope (Zeiss). Files were coded and processed by an investigator blind to status of the experiment. Larvae were collected for independent *post hoc* genotyping at the conclusion of image acquisition. Images were analyzed by a third investigator using DanioScope software (Noldus, version 1.0.109). Standard head (overall head length, midbrain and forebrain widths) and body length (distance from anterior tip of head to base of caudal fin) measurements were obtained. Files were un-coded and combined with genotyping data at the end of this process.

Interneuron Quantification

For imaging studies, *arxa* CRISPR line was crossed with a *dlx5a-dlx6a:GFP:nacre* transgenic zebrafish line provided by Marc Ekker[52]. For analysis of interneuron density in *arxa* WT and homozygote mutants, green fluorescent protein (GFP)-expressing larvae were sorted by fluorescence at 2 to 3 dpf and imaged at 5 dpf using a Zeiss Z.1 light sheet microscope with a 20X objective. Zebrafish were anesthetized in 0.04% tricaine mesylate and embedded in 2% low melting point agarose inside a glass capillary. The imaging sample chamber was filled with embryo medium. Z-stack images were acquired at 5 μm intervals starting at the first visible dorsal GFP-positive cell. Following image acquisition, larvae were gently removed from agar and independently genotyped. Imaging files were coded and analyzed *post hoc* by an investigator blind to status of the experiment. Images were then processed in Fiji (ImageJ)[78]. Neurons were quantified with an algorithm modified from "3D watershed technique" (ImageJ macro developed by [Bindokas V, 17-September-2014. Available: https://digital.bsd.uchicago.edu/%5Cimagej_macros.html.]).

Statistical analysis

Statistical tests were performed using MATLAB or GraphPad Prism. One-way ANOVA with Dunnett's multiple comparison tests or non-parametric *t* tests were used. Data are presented as mean ± S.E.M. Individual analyses are described in Results.

Data and software availability

All custom MATLAB programs will be made available upon reasonable request. Representative electrophysiology tracings, Kaplan-Meier survival plots, behavioral data, sequencing information are available on our web-portal (https://zebrafishproject.ucsf.edu). The datasets generated during the current studies are available from the corresponding author on reasonable request.

Reporting summary

Further information on research design is available in the Nature Research Reporting Summary linked to this article.

Ethics declarations

Competing interests

S.C.B. is a co-Founder and Scientific Advisor for EpyGenix Therapeutics. S.C.B. is on the Scientific Advisory Board of ZeClinics. The remaining authors declare that the research was conducted in the absence of any commercial or financial relationships that could be construed as a potential conflict of interest.

Acknowledgements

We would like to thank Dan Lowenstein, Gemma Carvill and Robert Hunt for comments and feedback on conceptualization of the Epilepsy Zebrafish Project. We thank Kathryn Salvati and Mark Beenhakker for sharing MATLAB code for generation of time-frequency histograms. We thank Sarai Diaz and Ifechukwu Okeke for assistance on maintenance of zebrafish lines. This work was supported by NIH/NINDS R01 award #NS103139 (to S.C.B.); International Foundation for CDKL5 Research and Bow Foundation grants (to S.C.B); Lennox-Gastaut Syndrome Foundation fellowships (to B.G. and C.C); and a Dravet Syndrome Foundation fellowship (to A.G.).

Author Contributions

A.G. & S.C.B. conceived the project. A.G. & C.C. designed the CRISPR strategy and trained subsequent personnel on generation of mutant lines. A.G. & C.C. directed and supervised the research. A.G., C.C., J.L., B.G., & K.H. generated mutant zebrafish lines. A.G., K.H. & M.A. conducted the gene expression studies. C.C. designed and guided the behavioral assay studies. C.C. & C.O. collected the behavioral data and C.C., C.O. & R. P. analyzed the data. S.C.B., M.M., & M.T.D. collected and analyzed electrophysiology data. T.Q. & J.L. collected and analyzed light sheet microscopy data. C.C., M.M., & F.F. collected and analyzed survival data. J.L. & R.P. designed and wrote MATLAB programs for data analysis. M.M. & C.O. created the database website. M.T.D., M.A., C.O. & F.F. maintained the zebrafish colony. A.G., C.C. & S.C.B. wrote and edited the paper.

Additional information

Supplementary Information is available for this paper.

Correspondence and requests for materials should be addressed to Scott C. Baraban (scott.baraban@ucsf.edu)

References

1 Shields, W. D. Catastrophic epilepsy in childhood. *Epilepsia* **41 Suppl 2**, S2-6, doi:10.1111/j.1528-1157.2000.tb01518.x (2000).

2 Camfield, P. & Camfield, C. Epileptic syndromes in childhood: clinical features, outcomes, and treatment. *Epilepsia* **43 Suppl 3**, 27-32, doi:10.1046/j.1528-1157.43.s.3.3.x (2002).

3 Katsnelson, A., Buzsáki, G. & Swann, J. W. Catastrophic childhood epilepsy: a recent convergence of basic and clinical neuroscience. *Sci Transl Med* **6**, 262ps213, doi:10.1126/scitranslmed.3010531 (2014).

4 Pal, D. K., Pong, A. W. & Chung, W. K. Genetic evaluation and counseling for epilepsy. *Nat Rev Neurol* **6**, 445-453, doi:10.1038/nrneurol.2010.92 (2010).

5 Myers, C. T. & Mefford, H. C. Advancing epilepsy genetics in the genomic era. *Genome Med* **7**, 91, doi:10.1186/s13073-015-0214-7 (2015).

6 Perucca, P. & Perucca, E. Identifying mutations in epilepsy genes: Impact on treatment selection. *Epilepsy Res* **152**, 18-30, doi:10.1016/j.eplepsyres.2019.03.001 (2019).

7 Hamdan, F. F. *et al.* High Rate of Recurrent De Novo Mutations in Developmental and Epileptic Encephalopathies. *Am J Hum Genet* **101**, 664-685, doi:10.1016/j.ajhg.2017.09.008 (2017).

690 8 Epi4K Consortium *et al.* De novo mutations in epileptic encephalopathies. *Nature* **501**,
691 217-221, doi:10.1038/nature12439 (2013).
692 9 Mastrangelo, M. & Leuzzi, V. Genes of early-onset epileptic encephalopathies: from
693 genotype to phenotype. *Pediatr Neurol* **46,** 24-31,
694 doi:10.1016/j.pediatneurol.2011.11.003 (2012).
695 10 Epilepsy Genetics Initiative. The Epilepsy Genetics Initiative: Systematic reanalysis of
696 diagnostic exomes increases yield. *Epilepsia* **60,** 797-806, doi: 10.1111/epi.14698 (2018).
697 11 EpiPM Consortium. A roadmap for precision medicine in the epilepsies. *Lancet Neurol*
698 **14,** 1219-1228, doi:10.1016/$1474-4422(15)00199-4 (2015).
699 12 Howe, K. *et al.* The zebrafish reference genome sequence and its relationship to the
700 human genome. *Nature* **496**, 498-503, doi:10.1038/nature12111 (2013).
701 13 Liu, J. *et al.* CRISPR/Cas9 in zebrafish: an efficient combination for human genetic
702 diseases modeling. *Hum Genet* **136**, 1-12, doi:10.1007/s00439-016-1739-6 (2017).
703 14 Adamson, K. I., Sheridan, E. & Grierson, A. J. Use of zebrafish models to investigate rare
704 human disease. *J Med Genet* **55**, 641-649, doi:10.1136/jmedgenet-2018-105358 (2018).
705 15 Liu, C. X. *et al.* CRISPR/Cas9-induced shank3b mutant zebrafish display autism-like
706 behaviors. *Mol Autism* **9**, 23, doi:10.1186/s13229-018-0204-x (2018).
707 16 Thyme, S. B. *et al.* Phenotypic Landscape of Schizophrenia-Associated Genes Defines
708 Candidates and Their Shared Functions. *Cell* **177**, 478-491.e420,
709 doi:10.1016/j.cell.2019.01.048 (2019).
710 17 Tang, W. *et al.* Genetic Control of Collective Behavior in Zebrafish. *iScience* **23**, 100942,
711 doi:10.1016/j.isci.2020.100942 (2020).
712 18 Vaz, R., Hofmeister, W. & Lindstrand, A. Zebrafish Models of Neurodevelopmental
713 Disorders: Limitations and Benefits of Current Tools and Techniques. *Int J Mol Sci* **20**,
714 doi:10.3390/ijms20061296 (2019).
715 19 Sakai, C., Ijaz, S. & Hoffman, E. J. Zebrafish Models of Neurodevelopmental Disorders:
716 Past, Present, and Future. *Front Mol Neurosci* **11**, 294, doi:10.3389/fnmol.2018.00294
717 (2018).
718 20 Gupta, T. *et al.* Morphometric analysis and neuroanatomical mapping of the zebrafish
719 brain. *Methods* **150**, 49-62, doi:10.1016/j.ymeth.2018.06.008 (2018).
720 21 Khan, K. M. *et al.* Zebrafish models in neuropsychopharmacology and CNS drug
721 discovery. *Br J Pharmacol* **174**, 1925-1944, doi:10.1111/bph.13754 (2017).
722 22 Cornet, C., Di Donato, V. & Terriente, J. Combining Zebrafish and CRISPR/Cas9: Toward a
723 More Efficient Drug Discovery Pipeline. *Front Pharmacol* **9**, 703,
724 doi:10.3389/fphar.2018.00703 (2018).
725 23 Baraban, S. C., Dinday, M. T. & Hortopan, G. A. Drug screening in Scn1a zebrafish mutant
726 identifies clemizole as a potential Dravet syndrome treatment. *Nat Commun* **4**, 2410,
727 doi:10.1038/ncomms3410 (2013).
728 24 Griffin, A. *et al.* Clemizole and modulators of serotonin signalling suppress seizures in
729 Dravet syndrome. *Brain* **140**, 669-683, doi:10.1093/brain/aww342 (2017).
730 25 Cully, M. Zebrafish earn their drug discovery stripes. *Nat Rev Drug Discov* **18**, 811-813,
731 doi:10.1038/d41573-019-00165-x (2019).

26 Weuring, W. J. *et al.* NaV1.1 and NaV1.6 selective compounds reduce the behavior phenotype and epileptiform activity in a novel zebrafish model for Dravet Syndrome. *PloS one* **15**, e0219106-e0219106, doi:10.1371/journal.pone.0219106 (2020).
27 Dinday, M. T. & Baraban, S. C. Large-Scale Phenotype-Based Antiepileptic Drug Screening in a Zebrafish Model of Dravet Syndrome. *eNeuro* **2**, doi:10.1523/eneuro.0068-15.2015 (2015).
28 Thornton, C., Dickson, K. E., Carty, D. R., Ashpole, N. M. & Willett, K. L. Cannabis constituents reduce seizure behavior in chemically-induced and scn1a-mutant zebrafish. *Epilepsy Behav* **110**, 107152, doi:10.1016/j.yebeh.2020.107152 (2020).
29 Griffin, A., Anvar, M., Hamling, K. & Baraban, S. C. Phenotype-Based Screening of Synthetic Cannabinoids in a Dravet Syndrome Zebrafish Model. *Front Pharmacol* **11**, 464, doi:10.3389/fphar.2020.00464 (2020).
30 Epilepsy, C. o. C. a. T. o. t. I. L. A. Proposal for revised clinical and electroencephalographic classification of epileptic seizures. From the Commission on Classification and Terminology of the International League Against Epilepsy. *Epilepsia* **22**, 489-501, doi:10.1111/j.1528-1157.1981.tb06159.x (1981).
31 Engel, J., Jr. A proposed diagnostic scheme for people with epileptic seizures and with epilepsy: report of the ILAE Task Force on Classification and Terminology. *Epilepsia* **42**, 796-803, doi:10.1046/j.1528-1157.2001.10401.x (2001).
32 Berg, A. T. *et al.* Revised terminology and concepts for organization of seizures and epilepsies: report of the ILAE Commission on Classification and Terminology, 2005-2009. *Epilepsia* **51**, 676-685, doi:10.1111/j.1528-1167.2010.02522.x (2010).
33 Fisher, R. S. *et al.* Operational classification of seizure types by the International League Against Epilepsy: Position Paper of the ILAE Commission for Classification and Terminology. *Epilepsia* **58**, 522-530, doi:10.1111/epi.13670 (2017).
34 Akman, O. *et al.* Methodologic recommendations and possible interpretations of video-EEG recordings in immature rodents used as experimental controls: A TASK1-WG2 report of the ILAE/AES Joint Translational Task Force. *Epilepsia Open* **3**, 437-459, doi:10.1002/epi4.12262 (2018).
35 Grone, B. P. & Baraban, S. C. Animal models in epilepsy research: legacies and new directions. *Nat Neurosci* **18**, 339-343, doi:10.1038/nn.3934 (2015).
36 Wong, M. & Roper, S. N. Genetic animal models of malformations of cortical development and epilepsy. *J Neurosci Methods* **260**, 73-82, doi:10.1016/j.jneumeth.2015.04.007 (2016).
37 Demarest, S. T. & Brooks-Kayal, A. From molecules to medicines: the dawn of targeted therapies for genetic epilepsies. *Nat Rev Neurol* **14**, 735-745, doi:10.1038/s41582-018-0099-3 (2018).
38 Yang, Y. & Frankel, W. N. Genetic approaches to studying mouse models of human seizure disorders. *Adv Exp Med Biol* **548**, 1-11, doi:10.1007/978-1-4757-6376-8_1 (2004).
39 Hwang, W. Y. *et al.* Heritable and precise zebrafish genome editing using a CRISPR-Cas system. *PLoS One* **8**, e68708, doi:10.1371/journal.pone.0068708 (2013).
40 Hwang, W. Y. *et al.* Efficient genome editing in zebrafish using a CRISPR-Cas system. *Nat Biotechnol* **31**, 227-229, doi:10.1038/nbt.2501 (2013).

41 Allen, A. S. *et al.* De novo mutations in epileptic encephalopathies. *Nature* **501**, 217-221, doi:10.1038/nature12439 (2013).

42 Grone, B. P. *et al.* Epilepsy, Behavioral Abnormalities, and Physiological Comorbidities in Syntaxin-Binding Protein 1 (STXBP1) Mutant Zebrafish. *PLoS One* **11**, e0151148, doi:10.1371/journal.pone.0151148 (2016).

43 Baraban, S. C. Forebrain electrophysiological recording in larval zebrafish. *J Vis Exp*, doi:10.3791/50104 (2013).

44 Baraban, S. C., Taylor, M. R., Castro, P. A. & Baier, H. Pentylenetetrazole induced changes in zebrafish behavior, neural activity and c-fos expression. *Neuroscience* **131**, 759-768, doi:10.1016/j.neuroscience.2004.11.031 (2005).

45 Baraban, S. C. *et al.* A large-scale mutagenesis screen to identify seizure-resistant zebrafish. *Epilepsia* **48**, 1151-1157, doi:10.1111/j.1528-1167.2007.01075.x (2007).

46 Pena, I. A. *et al.* Pyridoxine-Dependent Epilepsy in Zebrafish Caused by Aldh7a1 Deficiency. *Genetics* **207**, 1501-1518, doi:10.1534/genetics.117.300137 (2017).

47 Hunyadi, B., Siekierska, A., Sourbron, J., Copmans, D. & de Witte, P. A. M. Automated analysis of brain activity for seizure detection in zebrafish models of epilepsy. *J Neurosci Methods* **287**, 13-24, doi:10.1016/j.jneumeth.2017.05.024 (2017).

48 Koutroumanidis, M. *et al.* The role of EEG in the diagnosis and classification of the epilepsy syndromes: a tool for clinical practice by the ILAE Neurophysiology Task Force (Part 1). *Epileptic Disord* **19**, 233-298, doi:10.1684/epd.2017.0935 (2017).

49 Kato, M. & Dobyns, W. B. X-linked lissencephaly with abnormal genitalia as a tangential migration disorder causing intractable epilepsy: proposal for a new term, "interneuronopathy". *J Child Neurol* **20**, 392-397, doi:10.1177/08830738050200042001 (2005).

50 Marsh, E. D. *et al.* Developmental interneuron subtype deficits after targeted loss of Arx. *BMC Neurosci* **17**, 35, doi:10.1186/s12868-016-0265-8 (2016).

51 Friocourt, G. & Parnavelas, J. G. Mutations in ARX Result in Several Defects Involving GABAergic Neurons. *Front Cell Neurosci* **4**, 4, doi:10.3389/fncel.2010.00004 (2010).

52 Yu, M. *et al.* Activity of dlx5a/dlx6a regulatory elements during zebrafish GABAergic neuron development. *Int J Dev Neurosci* **29**, 681-691, doi:10.1016/j.ijdevneu.2011.06.005 (2011).

53 McLachlan, F., Sires, A. M. & Abbott, C. M. The role of translation elongation factor eEF1 subunits in neurodevelopmental disorders. *Hum Mutat* **40**, 131-141, doi:10.1002/humu.23677 (2019).

54 Papandreou, A. *et al.* GABRB3 mutations: a new and emerging cause of early infantile epileptic encephalopathy. *Dev Med Child Neurol* **58**, 416-420, doi:10.1111/dmcn.12976 (2016).

55 Zabinyakov, N. *et al.* Characterization of the first knock-out aldh7a1 zebrafish model for pyridoxine-dependent epilepsy using CRISPR-Cas9 technology. *PLOS ONE* **12**, e0186645, doi:10.1371/journal.pone.0186645 (2017).

56 Leu, C. *et al.* Polygenic burden in focal and generalized epilepsies. *Brain* **142**, 3473-3481, doi:10.1093/brain/awz292 (2019).

57 Henshall, D. C. & Kobow, K. Epigenetics and Epilepsy. *Cold Spring Harb Perspect Med* **5**, doi:10.1101/cshperspect.a022731 (2015).

58 Zhang, Y. H. *et al.* Genetic epilepsy with febrile seizures plus: Refining the spectrum. *Neurology* **89**, 1210-1219, doi:10.1212/wnl.0000000000004384 (2017).
59 Amendola, E. *et al.* Mapping pathological phenotypes in a mouse model of CDKL5 disorder. *PLoS One* **9**, e91613, doi:10.1371/journal.pone.0091613 (2014).
60 Wang, I. T. *et al.* Loss of CDKL5 disrupts kinome profile and event-related potentials leading to autistic-like phenotypes in mice. *Proc Natl Acad Sci U S A* **109**, 21516-21521, doi:10.1073/pnas.1216988110 (2012).
61 Kim, Y. J. *et al.* Chd2 Is Necessary for Neural Circuit Development and Long-Term Memory. *Neuron* **100**, 1180-1193.e1186, doi:10.1016/j.neuron.2018.09.049 (2018).
62 Yuskaitis, C. J. *et al.* A mouse model of DEPDC5-related epilepsy: Neuronal loss of Depdc5 causes dysplastic and ectopic neurons, increased mTOR signaling, and seizure susceptibility. *Neurobiol Dis* **111**, 91-101, doi:10.1016/j.nbd.2017.12.010 (2018).
63 Zaman, T., Abou Tayoun, A. & Goldberg, E. M. A single-center SCN8A-related epilepsy cohort: clinical, genetic, and physiologic characterization. *Ann Clin Transl Neurol* **6**, 1445-1455, doi:10.1002/acn3.50839 (2019).
64 Kolc, K. L. *et al.* A systematic review and meta-analysis of 271 PCDH19-variant individuals identifies psychiatric comorbidities, and association of seizure onset and disease severity. *Mol Psychiatry* **24**, 241-251, doi:10.1038/s41380-018-0066-9 (2019).
65 Borlot, F., Whitney, R., Cohn, R. D. & Weiss, S. K. MEF2C-related epilepsy: Delineating the phenotypic spectrum from a novel mutation and literature review. *Seizure* **67**, 86-90, doi:10.1016/j.seizure.2019.03.015 (2019).
66 Mirzaa, G. M. *et al.* CDKL5 and ARX mutations in males with early-onset epilepsy. *Pediatr Neurol* **48**, 367-377, doi:10.1016/j.pediatrneurol.2012.12.030 (2013).
67 Scheldeman, C. *et al.* mTOR-related neuropathology in mutant tsc2 zebrafish: Phenotypic, transcriptomic and pharmacological analysis. *Neurobiol Dis* **108**, 225-237, doi:10.1016/j.nbd.2017.09.004 (2017).
68 Liao, M. *et al.* Targeted knockout of GABA-A receptor gamma 2 subunit provokes transient light-induced reflex seizures in zebrafish larvae. *Dis Model Mech* **12**, doi:10.1242/dmm.040782 (2019).
69 Fuller, T. D., Westfall, T. A., Das, T., Dawson, D. V. & Slusarski, D. C. High-throughput behavioral assay to investigate seizure sensitivity in zebrafish implicates ZFHX3 in epilepsy. *J Neurogenet* **32**, 92-105, doi:10.1080/01677063.2018.1445247 (2018).
70 Hoffman, E. J. *et al.* Estrogens Suppress a Behavioral Phenotype in Zebrafish Mutants of the Autism Risk Gene, CNTNAP2. *Neuron* **89**, 725-733, doi:10.1016/j.neuron.2015.12.039 (2016).
71 Brueggeman, L. *et al.* Drug repositioning in epilepsy reveals novel antiseizure candidates. *Ann Clin Transl Neurol* **6**, 295-309, doi:10.1002/acn3.703 (2019).
72 Teng, Y. *et al.* Knockdown of zebrafish Lgi1a results in abnormal development, brain defects and a seizure-like behavioral phenotype. *Hum Mol Genet* **19**, 4409-4420, doi:10.1093/hmg/ddq364 (2010).
73 Samarut, É. *et al.* γ-Aminobutyric acid receptor alpha 1 subunit loss of function causes genetic generalized epilepsy by impairing inhibitory network neurodevelopment. *Epilepsia* **59**, 2061-2074, doi:10.1111/epi.14576 (2018).

74 Liu, F. *et al.* A novel LGI1 missense mutation causes dysfunction in cortical neuronal migration and seizures. *Brain Res* **1721**, 146332, doi:10.1016/j.brainres.2019.146332 (2019).

75 Pasquier, J. *et al.* Gene evolution and gene expression after whole genome duplication in fish: the PhyloFish database. *BMC Genomics* **17**, 368, doi:10.1186/s12864-016-2709-z (2016).

76 Mirat, O., Sternberg, J. R., Severi, K. E. & Wyart, C. ZebraZoom: an automated program for high-throughput behavioral analysis and categorization. *Front Neural Circuits* **7**, 107, doi:10.3389/fncir.2013.00107 (2013).

77 Lucore, E. C. & Connaughton, V. P. Observational learning and irreversible starvation in first-feeding zebrafish larvae: is it okay to copy from your friends? *Zoology* **145**, 125896, doi:https://doi.org/10.1016/j.zool.2021.125896 (2021).

78 Schindelin, J. *et al.* Fiji: an open-source platform for biological-image analysis. *Nat Methods* **9**, 676-682, doi:10.1038/nmeth.2019 (2012).

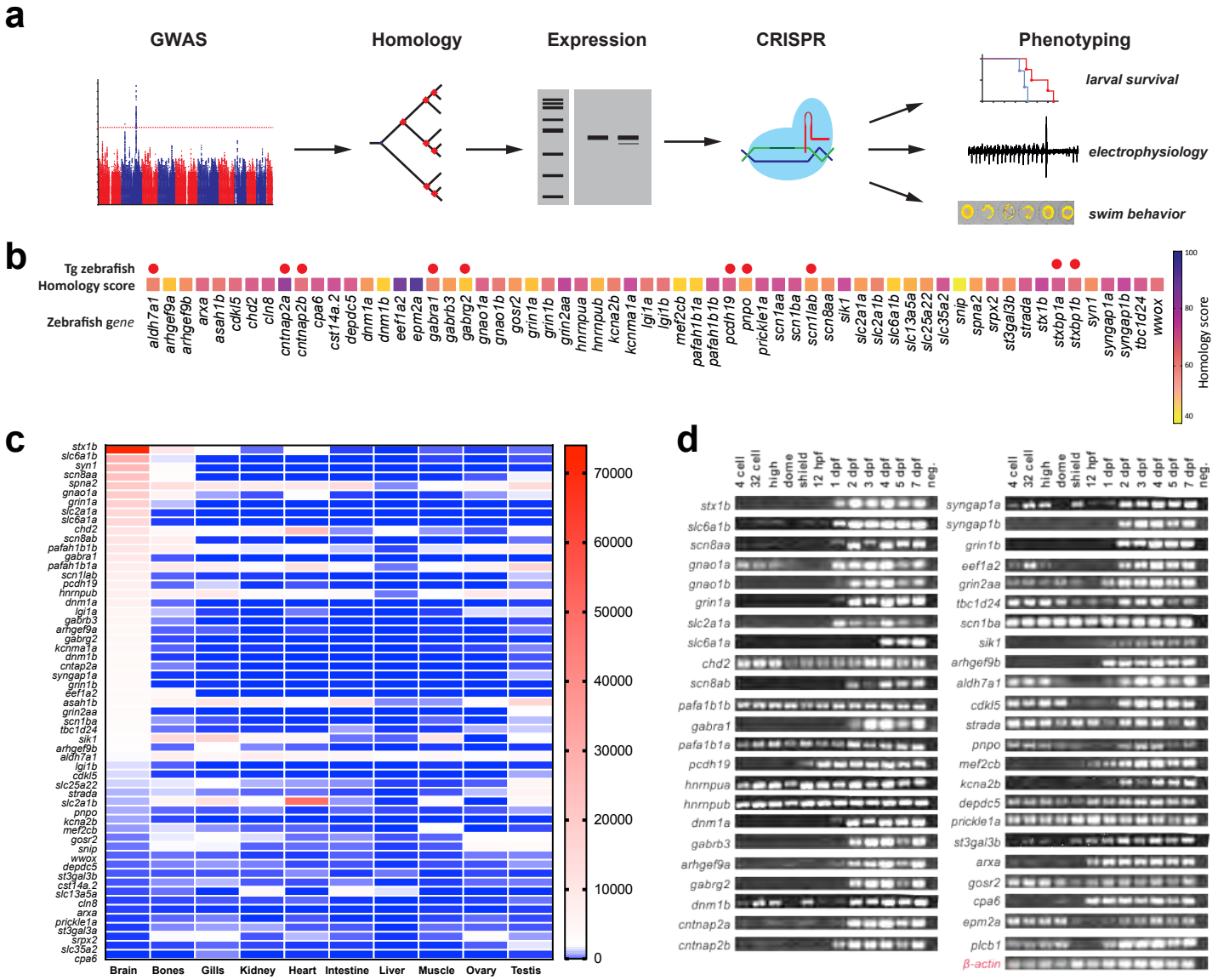
a
GWAS
Homology
Expression
CRISPR
Phenotyping
larval survival
electrophysiology
swim behavior
b
Tg zebrafish
Homology score
Zebrafish gene
aldh7a1 arhgef9a arhgef9b arxa asah1b cdkl5 chd2 cln8 cntnap2a cntnap2b cpa6 cst14a.2 depdc5 dnm1a dnm1b eef1a2 epm2a gabra1 gabrb3 gabrg2 gnao1a gnao1b gosr2 grin1a grin1b grin2aa hnrnpua hnrnpub kcna2b kcnma1a lgi1a lgi1b mef2cb pafah1b1a pafah1b1b pcdh19 pnpo prickle1a scn1aa scn1ba scn1lab scn8aa sik1 slc2a1a slc6a1b slc13a5a slc25a22 slc35a2 snip spna2 srpx2 st3gal3b strada stx1b stxbp1a stxbp1b syn1 syngap1a syngap1b tbc1d24 wwox
Homology score
100
80
60
40
c
stx1b slc6a1b syn1 scn8aa spna2 gnao1a grin1a slc2a1a slc6a1a chd2 scn8ab pafah1b1b gabra1 pafah1b1a scn1lab pcdh19 hnrnpub dnm1a lgi1a gabrb3 arhgef9a gabrg2 kcnma1a dnm1b cntap2a syngap1a grin1b eef1a2 asah1b grin2aa scn1ba tbc1d24 sik1 arhgef9b aldh7a1 lgi1b cdkl5 slc25a22 strada slc2a1b pnpo kcna2b mef2cb gosr2 snip wwox depdc5 st3gal3b cst14a.2 slc13a5a cln8 arxa prickle1a st3gal3a srpx2 slc35a2 cpa6
Brain Bones Gills Kidney Heart Intestine Liver Muscle Ovary Testis
70000
60000
50000
40000
30000
20000
10000
0
d
4 cell 32 cell high dome shield 12 hpf 1 dpf 2 dpf 3 dpf 4 dpf 5 dpf 7 dpf neg.
stx1b slc6a1b scn8aa gnao1a gnao1b grin1a slc2a1a slc6a1a chd2 scn8ab pafa1b1b gabra1 pafa1b1a pcdh19 hnrnpua hnrnpub dnm1a gabrb3 arhgef9a gabrg2 dnm1b cntnap2a cntnap2b
syngap1a syngap1b grin1b eef1a2 grin2aa tbc1d24 scn1ba sik1 arhgef9b aldh7a1 cdkl5 strada pnpo mef2cb kcna2b depdc5 prickle1a st3gal3b arxa gosr2 cpa6 epm2a plcb1 β-actin
e
depdc5 WT
GGAGTCAGTCAGCAGGAAGAGCTGGGGCTCTGCAGACGTGGGCAGCTCTCCTCCAAACCGCCATACAGGACCAG
depdc5 MUT
Δ -14
GGAGTCAGTCAGCAGGAAGAGCTGGGG----------GCAGCTCTCCTCCAAACCGCCATACAGGACCAG
eef1a2 WT
GGCTGGAAGCTGGACAGGAAGGAGCACCATGCCGGTGGTGTTACTCTATTGGAAGCTCTTGATACCATCATGCC
eef1a2 MUT
Δ -7
GGCTGGAAGCTGGACAGGAAGGAGCAC-------GTGGTGTTACTCTATTGGAAGCTCTTGATACCATCATGCC

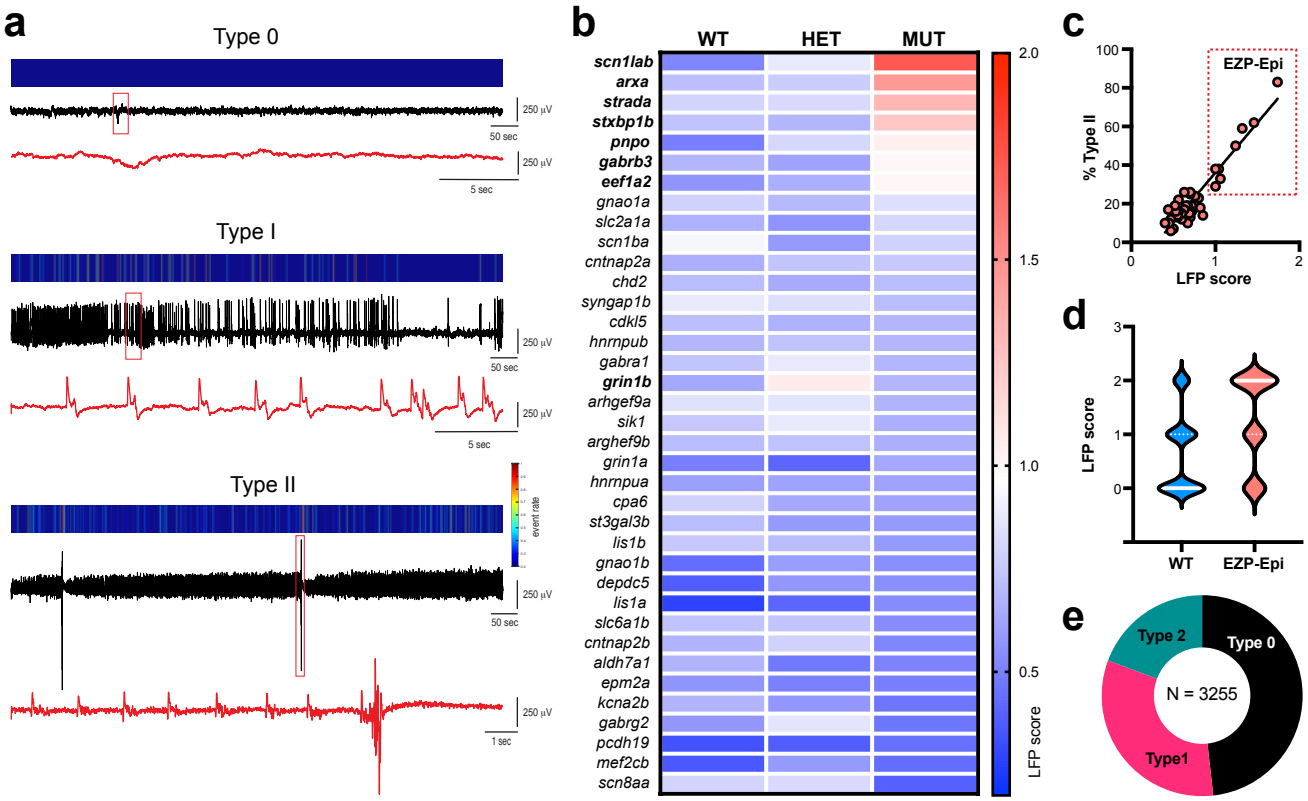
a
Type 0
250 µV
50 sec
250 µV
5 sec
Type I
250 µV
50 sec
250 µV
5 sec
Type II
event rate
250 µV
50 sec
250 µV
1 sec
b
WT
HET
MUT
scn1lab
arxa
strada
stxbp1b
pnpo
gabrb3
eef1a2
gnao1a
slc2a1a
scn1ba
cntnap2a
chd2
syngap1b
cdkl5
hnrnpub
gabra1
grin1b
arhgef9a
sik1
arghef9b
grin1a
hnrnpua
cpa6
st3gal3b
lis1b
gnao1b
depdc5
lis1a
slc6a1b
cntnap2b
aldh7a1
epm2a
kcna2b
gabrg2
pcdh19
mef2cb
scn8aa
2.0
1.5
1.0
0.5
LFP score
c
EZP-Epi
% Type II
100
80
60
40
20
0
0
1
2
LFP score
d
LFP score
3
2
1
0
WT
EZP-Epi
e
Type 2
Type 0
N = 3255
Type1

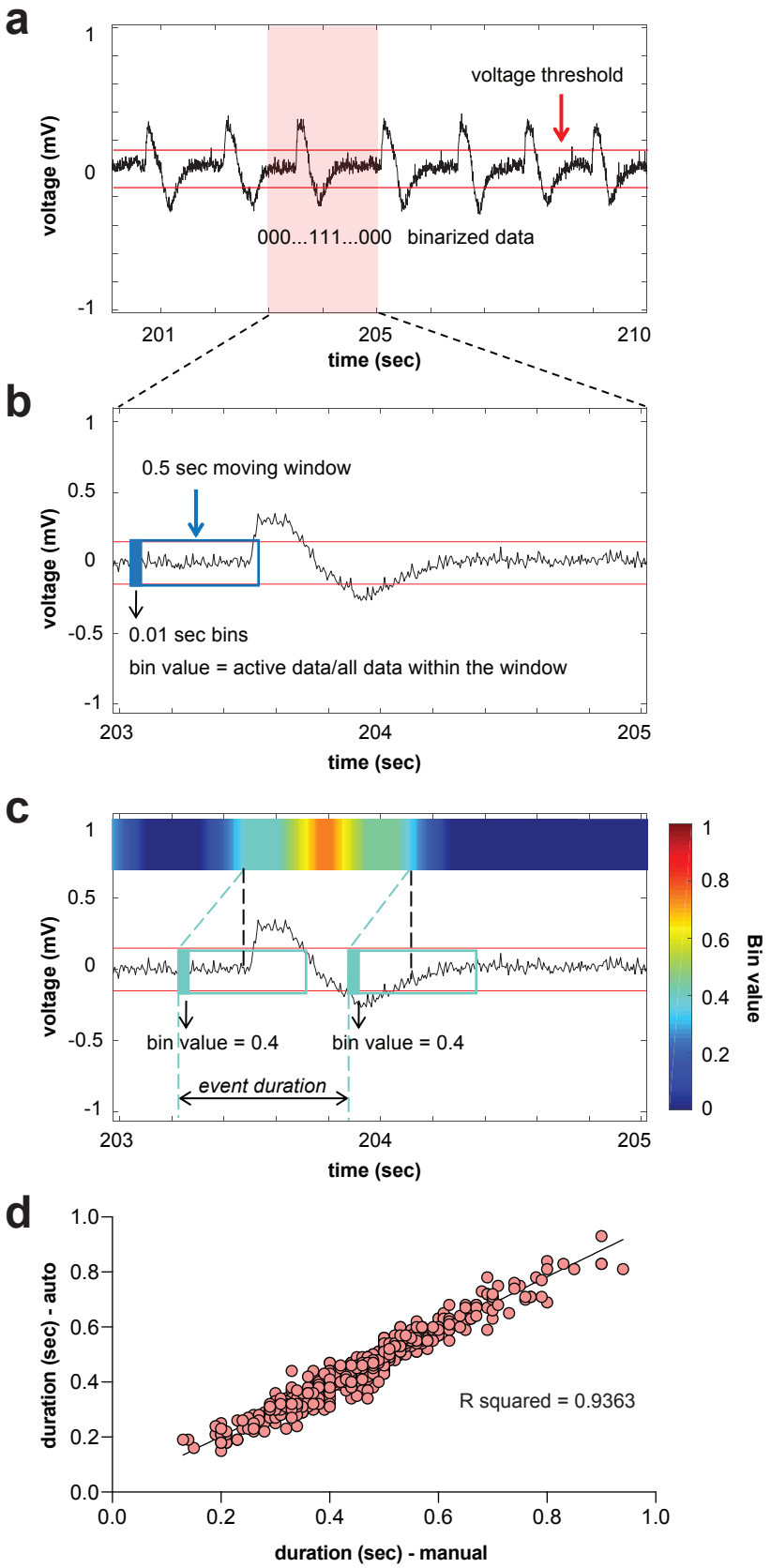
a
voltage threshold
000...111...000 binarized data
voltage (mV)
time (sec)
b
0.5 sec moving window
0.01 sec bins
bin value = active data/all data within the window
voltage (mV)
time (sec)
c
bin value = 0.4
bin value = 0.4
event duration
voltage (mV)
time (sec)
Bin value
d
R squared = 0.9363
duration (sec) - auto
duration (sec) - manual

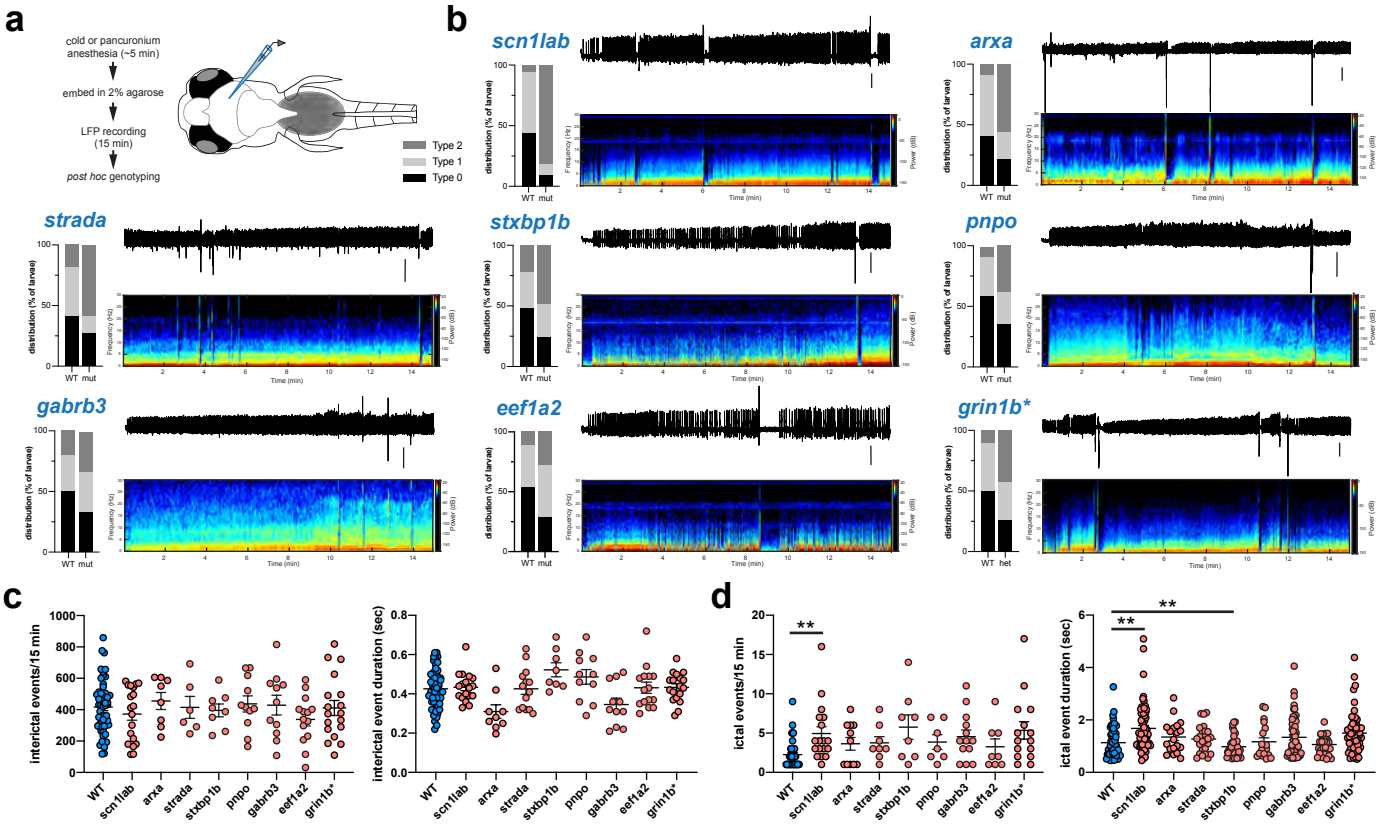
a
cold or pancuronium anesthesia (~5 min)
embed in 2% agarose
LFP recording (15 min)
post hoc genotyping
Type 2
Type 1
Type 0
b
scn1lab
arxa
strada
stxbp1b
pnpo
gabrb3
eef1a2
grin1b*
distribution (% of larvae)
WT
mut
het
Frequency (Hz)
Power (dB)
Time (min)
c
interictal events/15 min
interictal event duration (sec)
d
ictal events/15 min
ictal event duration (sec)
**
WT
scn1lab
arxa
strada
stxbp1b
pnpo
gabrb3
eef1a2
grin1b*

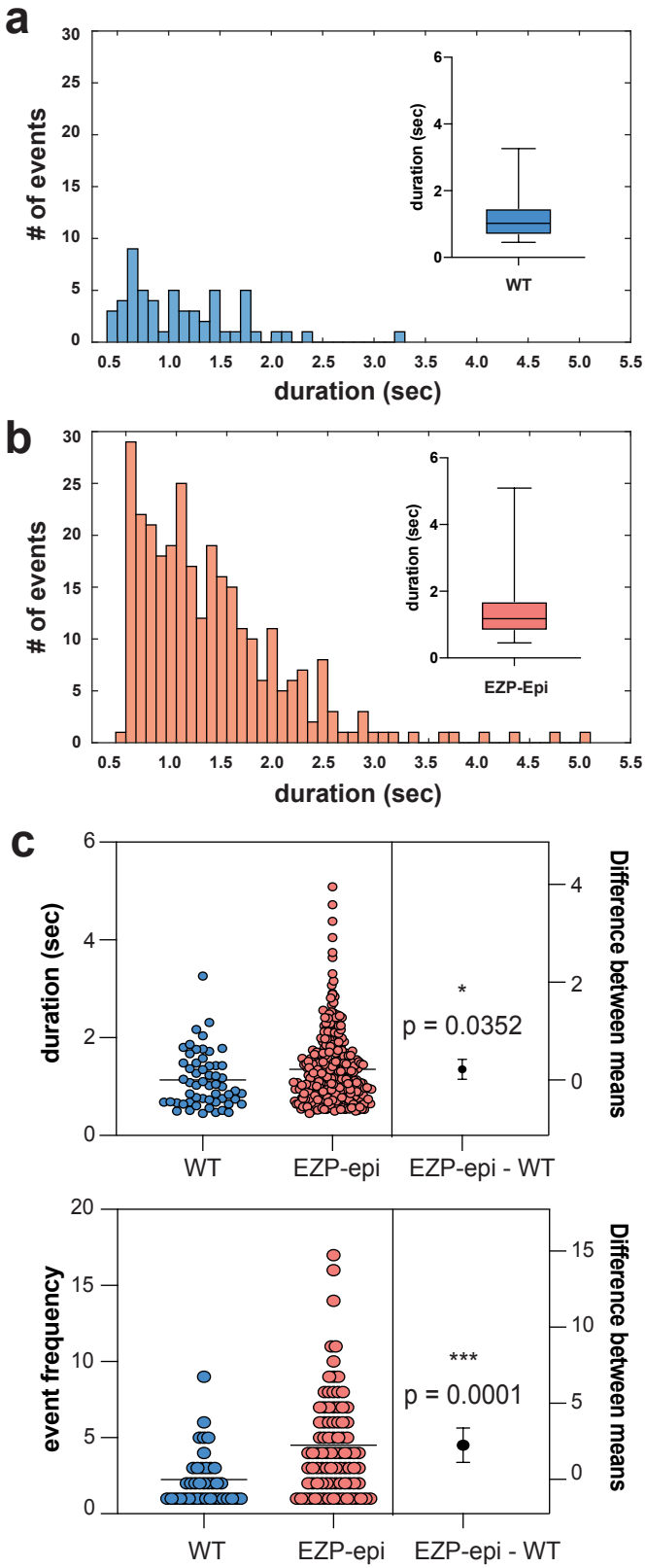
a
# of events
duration (sec)
duration (sec)
WT
b
# of events
duration (sec)
duration (sec)
EZP-Epi
c
duration (sec)
Difference between means
p = 0.0352
*
WT
EZP-epi
EZP-epi - WT
event frequency
Difference between means
p = 0.0001
***
WT
EZP-epi
EZP-epi - WT

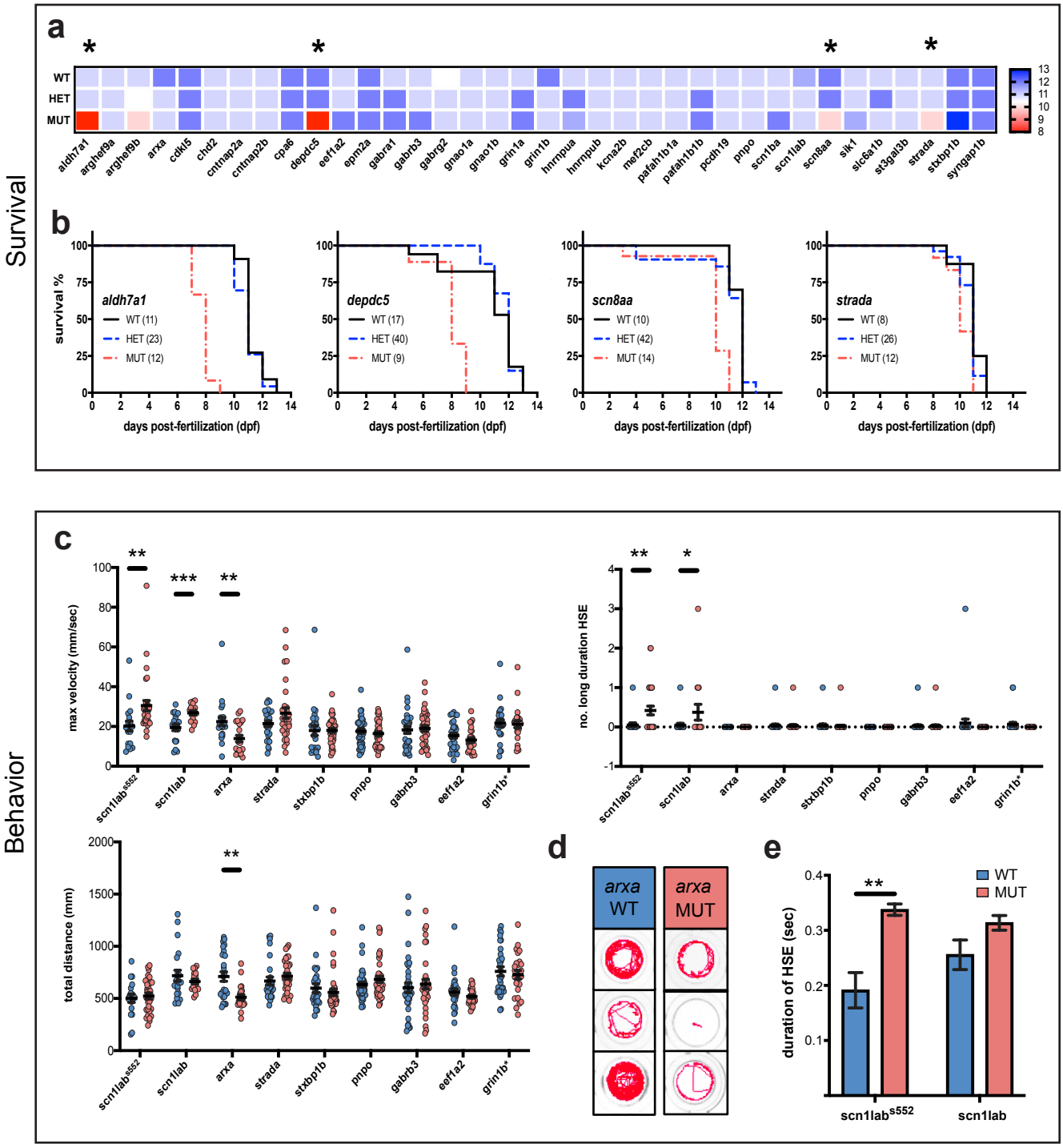
Survival
a
WT
HET
MUT
aldh7a1
arghef9a
arghef9b
arxa
cdkl5
chd2
cntnap2a
cntnap2b
cpa6
depdc5
eef1a2
epm2a
gabra1
gabrb3
gabrg2
gnao1a
gnao1b
grin1a
grin1b
hnrnpua
hnrnpub
kcna2b
mef2cb
pafah1b1a
pafah1b1b
pcdh19
pnpo
scn1ba
scn1lab
scn8aa
slk1
slc6a1b
st3gal3b
strada
stxbp1b
syngap1b
b
survival %
days post-fertilization (dpf)
aldh7a1
WT (11)
HET (23)
MUT (12)
depdc5
WT (17)
HET (40)
MUT (9)
scn8aa
WT (10)
HET (42)
MUT (14)
strada
WT (8)
HET (26)
MUT (12)
Behavior
c
max velocity (mm/sec)
no. long duration HSE
total distance (mm)
scn1lab552
scn1lab
arxa
strada
stxbp1b
pnpo
gabrb3
eef1a2
grin1b*
d
arxa WT
arxa MUT
e
duration of HSE (sec)
WT
MUT
scn1lab552
scn1lab

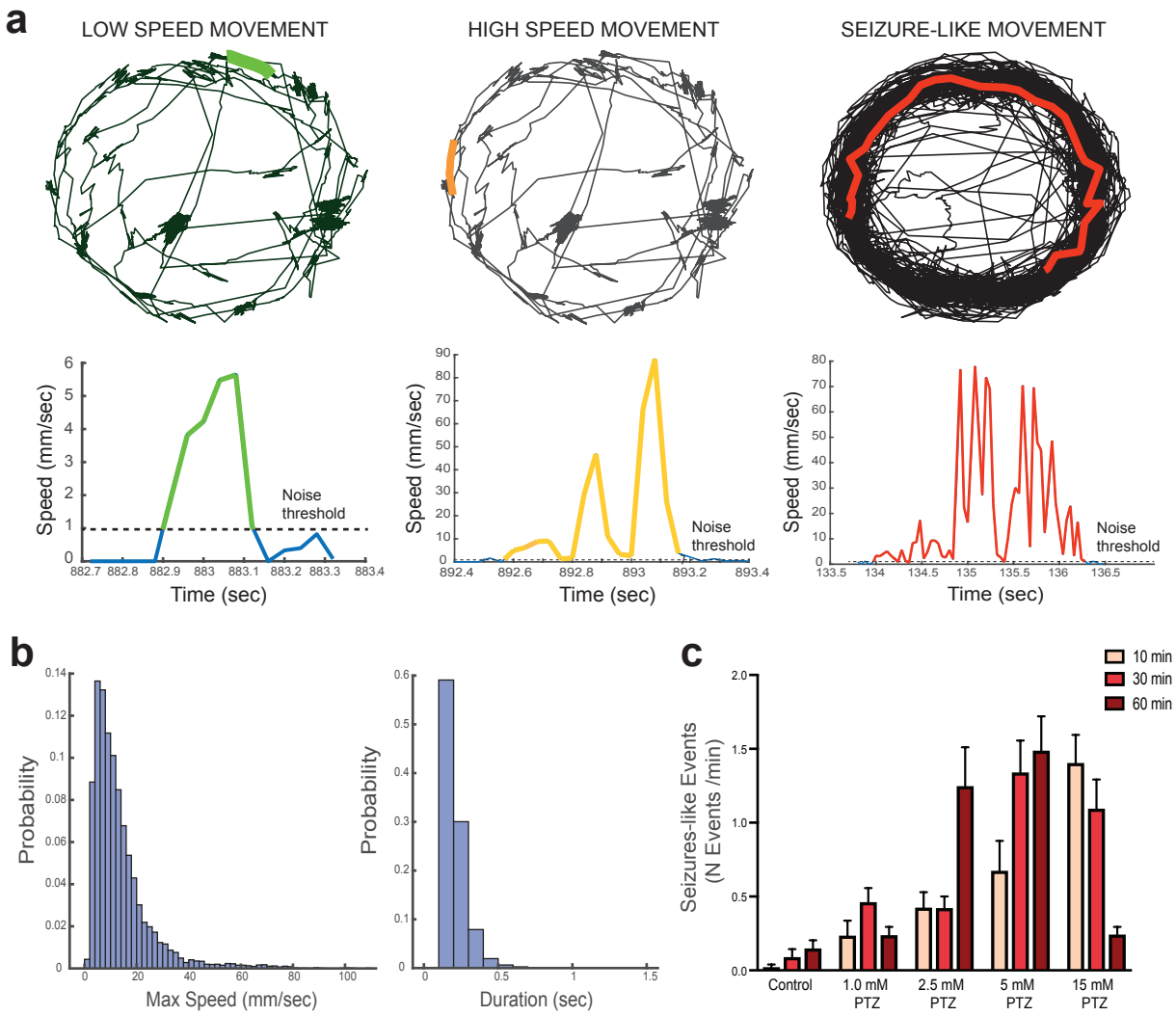
a
LOW SPEED MOVEMENT
HIGH SPEED MOVEMENT
SEIZURE-LIKE MOVEMENT
Speed (mm/sec)
Noise threshold
Time (sec)
b
Probability
Max Speed (mm/sec)
Duration (sec)
c
10 min
30 min
60 min
Seizures-like Events (N Events /min)
Control
1.0 mM PTZ
2.5 mM PTZ
5 mM PTZ
15 mM PTZ

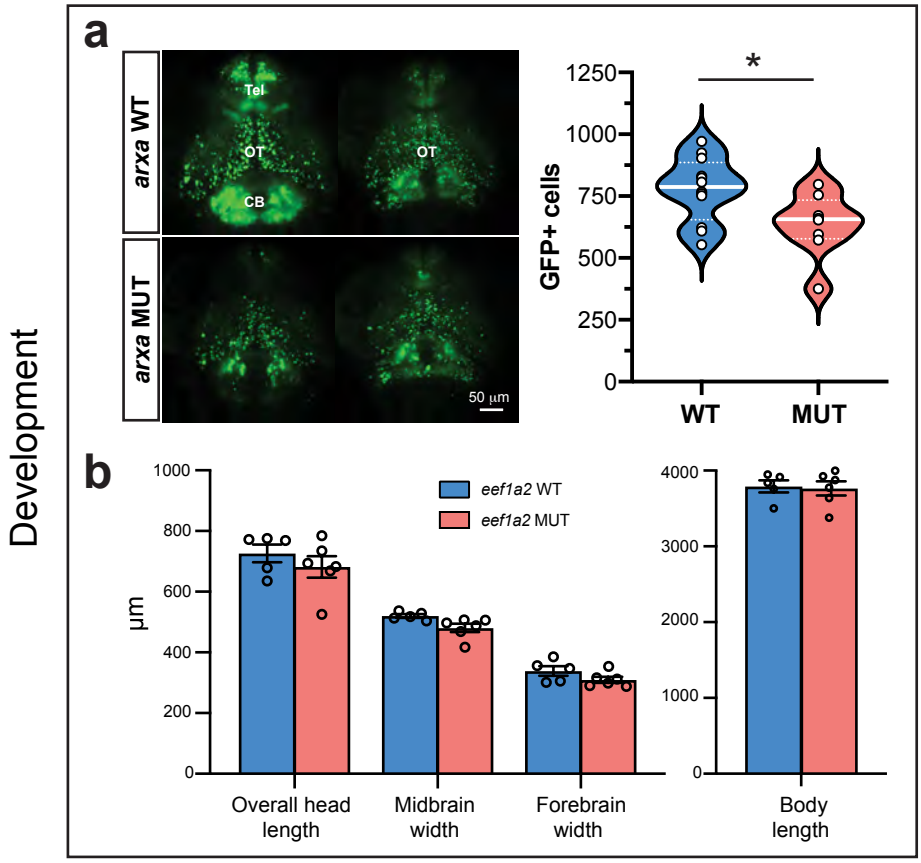
Development
a
arxa WT
arxa MUT
Tel
OT
OT
CB
50 µm
GFP+ cells
1250
1000
750
500
250
0
*
WT
MUT
b
µm
1000
800
600
400
200
0
eef1a2 WT
eef1a2 MUT
Overall head length
Midbrain width
Forebrain width
4000
3000
2000
1000
0
Body length

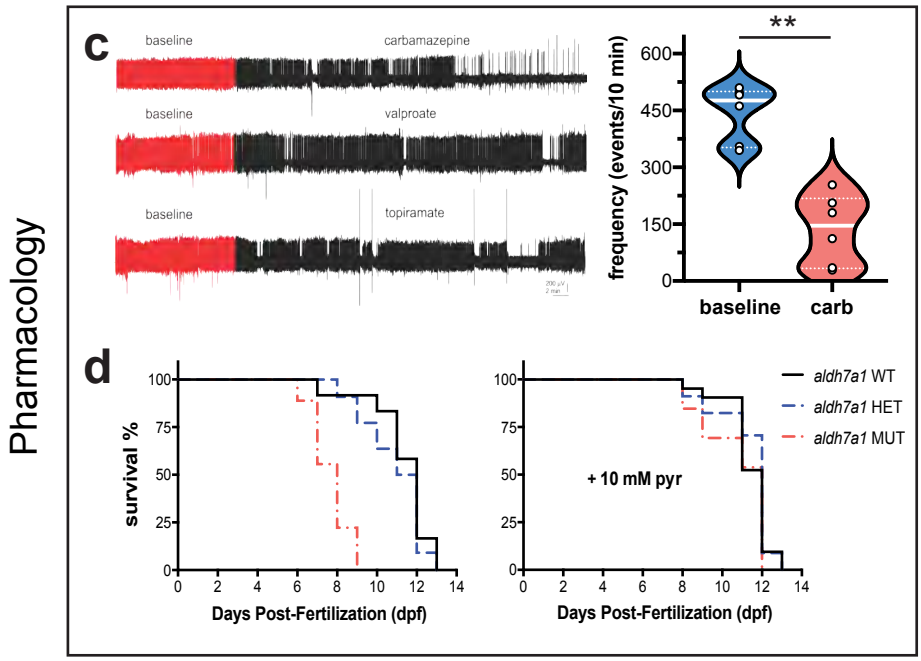
Pharmacology
c
baseline
carbamazepine
baseline
valproate
baseline
topiramate
frequency (events/10 min)
600
450
300
150
0
**
baseline
carb
d
survival %
100
75
50
25
0
0 2 4 6 8 10 12 14
Days Post-Fertilization (dpf)
+ 10 mM pyr
aldh7a1 WT
aldh7a1 HET
aldh7a1 MUT

Table S1: Genes associated with an epilepsy phenotype that were considered for the Epilepsy Zebrafish Project

Human Gene	OMIM	Phenotype	Inheritance	Mechanism
SCN1A	182389	Epileptic encephalopathy, early infantile (Dravet syndrome)	Autosomal dominant	LOF
SCN1B	600235	Atrial fibrillation, familial, 13	Autosomal dominant	LOF
		Brugada syndrome 5		
		Cardiac conduction defect, nonspecific		
		Epilepsy, generalized, with febrile seizures plus, type 1		
		Epileptic encephalopathy, early infantile, 52	Autosomal dominant	
SCN8A	600702	Cognitive impairment with or without cerebellar ataxia	Autosomal dominant	LOF
		Epileptic encephalopathy, early infantile, 13	Autosomal dominant	
		Seizures, benign familial infantile, 5	Autosomal dominant	
SCN9A	603415	Epilepsy, generalized, with febrile seizures plus, type 7	Autosomal dominant	n/a
		Erythermalgia, primary	Autosomal dominant	
		Febrile seizures, familial, 3B	Autosomal dominant	
		HSAN2D, autosomal recessive	Autosomal recessive	
		Insensitivity to pain, congenital	Autosomal recessive	
		Paroxysmal extreme pain disorder,	Autosomal dominant	
		Small fiber neuropathy	Autosomal dominant	
		{Dravet syndrome, modifier of}		
KCNA2	176262	Epileptic encephalopathy, early infantile, 32	Autosomal dominant	LOF
KCNMA1	600150	Cerebellar atrophy, developmental delay, and seizures	Autosomal dominant	
		Paroxysmal nonkinesigenic dyskinesia, 3, with or without generalized epilepsy		
KCNQ3	602232	Seizures, benign neonatal, type 2	Autosomal dominant	
KCTD1	613420	Scalp-ear-nipple syndrome	Autosomal dominant	
GABRA1	137160	Epileptic encephalopathy, early infantile	Autosomal dominant	LOF
GABRB3	137192	Epileptic encephalopathy, early infantile, 43	Autosomal dominant	LOF
		{Epilepsy, childhood absence, susceptibility to, 5}		
GABRG2	137164	Epilepsy, generalized, with febrile seizures plus, type 3	Autosomal dominant	LOF
		Febrile seizures, familial, 8		
		{Epilepsy, childhood absence, susceptibility to, 2}		
GRIN1	138249	Mental retardation, autosomal dominant 8	n/a	n/a
GRIN2A	138253	Epilepsy, focal, with speech disorder and with or without mental retardation	Autosomal dominant	LOF
SLC13A5	608305	Epileptic encephalopathy, early infantile, 25	Autosomal recessive	LOF
SLC25A22	609302	Epileptic encephalopathy, early infantile, 3	Autosomal recessive	LOF
SLC2A1	138140	Dystonia 9	Autosomal dominant	LOF
		GLUT1 deficiency syndrome 1, infantile onset, severe	Autosomal recessive Autosomal dominant	
		GLUT1 deficiency syndrome 2, childhood onset	Autosomal dominant	
		Stomatin-deficient cryohydrocytosis with neurologic defects	Autosomal dominant	
		{Epilepsy, idiopathic generalized, susceptibility to, 12}	Autosomal dominant	

SLC35A2	314375	Congenital disorder of glycosylation, type IIm	X-linked dominant; Somatic mosaicism	LOF
		Epileptic encephalopathy, early infantile, 22		
SLC6A1	137165	Myoclonic-atonic epilepsy	Autosomal dominant	LOF
DNM1	602377	Epileptic encephalopathy, early infantile, 31	Autosomal dominant	LOF
GOSR2	604027	Epilepsy, progressive myoclonic 6	Autosomal recessive	LOF
PRRT2	614386	Convulsions, familial infantile, with paroxysmal choreoathetosis	Autosomal dominant	LOF
		Episodic kinesigenic dyskinesia 1	Autosomal dominant	LOF
		Seizures, benign familial infantile, 2	Autosomal dominant	LOF
SPTAN1	182810	Epileptic encephalopathy, early infantile, 5	Autosomal dominant	
STX1B	601485	Generalized epilepsy with febrile seizures plus, type 9	Autosomal dominant	
STXBP1	602926	Epileptic encephalopathy, early infantile, 4	Autosomal dominant	
SYN1	313440	Epilepsy, X-linked, with variable learning disabilities and behavior disorders	X-linked recessive; X-linked dominant	
SYNGAP1	603384	Mental retardation, autosomal dominant 5	Autosomal dominant	
ARX	300382	Epileptic encephalopathy, early infantile, 1	X-linked recessive	LOF
		Hydranencephaly with abnormal genitalia	X-linked	
		Lissencephaly, X-linked 2	X-linked	
		Mental retardation, X-linked 29 and others	X-linked recessive	
		Partington syndrome	X-linked recessive	
		Proud syndrome	X-linked	
EEF1A2	602959	Epileptic encephalopathy, early infantile, 33	Autosomal dominant	n/a
		Mental retardation, autosomal dominant 38		
HNRNPU	602869	Epileptic encephalopathy, early infantile	Autosomal dominant	LOF
MEF2C	600662	Mental retardation, stereotypic movements, epilepsy, and/or cerebral malformations	Autosomal dominant	LOF
		Chromosome 5q14.3 deletion syndrome	Autosomal dominant	
PNKP	605610	Ataxia-oculomotor apraxia 4	Autosomal recessive	LOF
		Microcephaly, seizures, and developmental delay	Autosomal recessive	
PRICKLE1	608500	Epilepsy, progressive myoclonic 1B	Autosomal recessive	LOF
SNIP1	608241	Psychomotor retardation, epilepsy, and craniofacial dysmorphism	Autosomal recessive	LOF
CHD2	602119	Epileptic encephalopathy, childhood-onset	Autosomal dominant	LOF
ALDH7A1	107323	Epilepsy, pyridoxine-dependent	Autosomal recessive	LOF
PNPO	603287	Pyridoxamine 5'-phosphate oxidase deficiency	Autosomal recessive	LOF
WWOX	605131	Epileptic encephalopathy, early infantile, 28	Autosomal recessive	LOF
		Esophageal squamous cell carcinoma, somatic		
		Spinocrebellar ataxia, autosomal recessive 12	Autosomal recessive	
ALG13	300776	Epileptic encephalopathy, early infantile, 36	X-linked dominant	n/a
		Congenital disorder of glycosylation, type Is		
ASAH1	613468	Farber lipogranulomatosis	Autosomal recessive	LOF
		Spinal muscular atrophy with progressive myoclonic epilepsy	Autosomal recessive	LOF
CLN8	607837	Ceroid lipofuscinosis, neuronal, 8	Autosomal recessive	n/a
		Ceroid lipofuscinosis, neuronal, 8, Northern epilepsy variant	Autosomal recessive	

CDKL5	300203	Epileptic encephalopathy, early infantile, 2	X-linked dominant	LOF
EPM2A	607566	Epilepsy, progressive myoclonic 2A (Lafora)	Autosomal recessive	LOF
SIK1	605705	Epileptic encephalopathy, early infantile, 30	Autosomal dominant	n/a
STRADA	608626	Polyhydramnios, megalencephaly, and symptomatic epilepsy	Autosomal recessive	LOF
ARHGEF9	300429	Epileptic encephalopathy, early infantile, 8	X-linked recessive	LOF
DEPDC5	614191	Epilepsy, familial focal, with variable foci 1	Autosomal dominant	LOF
GNAO1	139311	Epileptic encephalopathy, early infantile, 17	Autosomal dominant	n/a
		Neurodevelopmental disorder with involuntary movements	Autosomal dominant	
PLCB1	607120	Epileptic encephalopathy, early infantile, 12	Autosomal recessive	LOF
TBC1D24	613577	Deafness, autosomal recessive 86	Autosomal recessive	
		Deafness, autosomal dominant 65	Autosomal dominant	
		DOOR syndrome	Autosomal recessive	LOF
		Epileptic encephalopathy, early infantile, 16	Autosomal recessive	LOF
		Myoclonic epilepsy, infantile, familial	Autosomal recessive	
CNTNAP2	604569	Cortical dysplasia-focal epilepsy syndrome	n/a	LOF
		Pitt-Hopkins like syndrome 1	n/a	
		{Autism susceptibility 15}	n/a	
LGI1	604619	Epilepsy, familial temporal lobe, 1	Autosomal dominant	LOF
PCDH19	300460	Epileptic encephalopathy, early infantile, 9	X-linked	LOF
RELN	600514	Lissencephaly 2 (Norman-Roberts type)	Autosomal recessive	LOF
		{Epilepsy, familial temporal lobe, 7}	Autosomal dominant	LOF
SRPX2	300642	(Rolandic epilepsy, mental retardation, and speech dyspraxia)	n/a	LOF
SZT2	615463	Epileptic encephalopathy, early infantile, 18	Autosomal recessive	LOF
PAFAH1B1	601545	Lissencephaly	Isolated cases	LOF
		Subcortical laminar heterotopia		
CPA6	609562	Epilepsy, familial temporal lobe, 5	Autosomal dominant; Autosomal recessive	LOF
		Febrile seizures, familial, 11		
CSTB	601145	Epilepsy, progressive myoclonic 1A (Unverricht and Lundborg syndrome)	Autosomal recessive	LOF
NHLRC1	608072	Epilepsy, progressive myoclonic 2B (Lafora)	Autosomal recessive	LOF
SCARB2	602257	Epilepsy, progressive myoclonic 4, with or without renal failure	Autosomal recessive	LOF
ST3GAL5	604402	Salt and pepper developmental regression syndrome	Autosomal recessive	LOF
ST3GAL3	138140	Autosomal Recessive Mental Retardation 12	Autosomal dominant	LOF
		Early Infantile Epileptic Encephalopathy 15		
KCNC1	616187	Epilepsy, progressive myoclonic 7	Autosomal dominant	n/a

Table S2: The 40 genes targeted for the Epilepsy Zebrafish Project.

Human gene	Zebrafish gene	Protein Sequence Reference	% protein identity (GRCz10)	% DIOPT	Homology Score
ALDH7A1	*aldh7a1*	ENSDARP00000108190	81	75	78
ARHGEF9	*arhgef9a*	ENSDARP00000118893	79	100	90
	arhgef9b	ENSDARP00000115968	84	75	80
ARX	*arxa*	ENSDARP00000075256	68	75	72
	arxb	not identified			
CDKL5	*cdkl5*	ENSDARP00000111280	54	92	73
CHD2	*chd2*	ENSDARP00000108411	73	67	70
CNTNAP2	*cntnap2a*	(ENSDART00000178326.1)	71	67	69
	cntnap2b	ENSDARP00000104097	65	50	58
CPA6	*cpa6*	ENSDARP00000096966	64	83	74
DEPDC5	*depdc5*	ENSDARP00000098526	75	58	67
DNM1	*dnm1a*	ENSDARP00000124266	89	50	70
	dnm1b	ENSDARP00000088100	88	75	82
EEF1A2	*eef1a2*	ENSDARP00000010921	92	92	92
EPM2A	*epm2a*	ENSDARP00000132560	62	42	52
GABRA1	*gabra1*	ENSDARP00000090772	84	92	88
GABRB3	*gabrb3*	ENSDARP00000081734	73	83	78
GABRG2	*gabrg2*	ENSDARP00000087253	83	83	83
GNAO1	*gnao1a*	ENSDARP00000124476	90	92	91
	gnao1b	ENSDARP00000052345	84	58	71
GOSR2	*gosr2*	ENSDARP00000069524	69	83	76
GRIN1	*grin1a*	ENSDARP00000093144	88	75	82
	grin1b	ENSDARP00000038151	88	92	90
GRIN2A	*grin2aa*	ENSDARP00000116766	67	83	75
	grin2ab	not identified			
HNRNPU	*hnrnpua*	ENSDARP00000144487	52	75	64
	hnrnpub	ENSDARP00000112099	57	83	70
KCNA2	*kcna2a*	not identified			
	kcna2b	ENSDARP00000130579	92	83	88
KCNMA1	*kcnma1a*	ENSDARP00000118939	87	67	77
MEF2C	*mef2ca*	not identified			
	mef2cb	ENSDARP00000138296	74	75	75
PAFAH1B1	*pafah1b1a*	ENSDARP00000042217	94	92	93
	pafah1b1b	ENSDARP00000039257	93	92	92
PCDH19	*pcdh19*	ENSDARP00000124001	70	67	68
PLCB1	*plcb1*	not identified			
PNPO	*pnpo*	ENSDARP00000011179	64	75	70
PRICKLE1	*prickle1a*	ENSDARP00000059513	69	100	85

	prickle1b	not identified			
SCN1B	*scn1ba*	ENSDARP00000079066	36	100	68
SCN1A	*scn1laa*	ENSDARP00000138437	67	67	67
	scn1lab	ENSDARP00000125843	77	58	68
SCN8A	*scn8aa*	ENSDARP00000024690	83	83	83
	scn8ab	ENSDARP00000126281	84	75	80
SIK1	*sik1*	ENSDARP00000077468	57	75	66
SLC2A1	*slc2a1a*	ENSDARP00000022579	74	92	83
SLC6A1	*slc6a1a*	ENSDARP00000119658	73	83	78
	slc6a1b	ENSDARP00000005281	84	100	92
SPTAN1	*spna2*	ENSDARP00000093027	90	83	87
ST3GAL3	*st3gal3b*	ENSDARP00000110277	63	100	82
STRADA	*strada*	ENSDARP00000115217	70	67	68
STX1B	*stx1b*	ENSDARP00000076389	97	100	99
STXBP1	*stxbp1a*	ENSDARP00000012776	85	83	84
	stxbp1b	ENSDARP00000026241	77	67	72
SYNGAP1	*syngap1a*	ENSDARP00000144044	63	75	69
	syngap1b	ENSDARP00000087797	63	67	65
TBC1D24	*tbc1d24*	ENSDARP00000128484	55	83	69

Table S3: Characterization of zebrafish orthologues for phenotypic characterization

Human	Zebrafish	Homology	Brain Expression	Development	Phenotypic Characterization
SCN1A	*scn1lab**				Y
	scn1laa				
SCN8A	*scn8aa*	*scn8aa*	*scn8aa*	*scn8aa*	Y
	scn8ab			*scn8ab*	
GABRA1	*gabra1*	*gabra1*	*gabra1*	*gabra1*	Y
GABRB3	*gabrb3*	*gabrb3*	*gabrb3*	*gabrb3*	Y
GABRG2	*gabrg2*	*gabrg2*	*gabrg2*	*gabrg2*	Y
GRIN2A	*grin2aa*	*grin2aa*	*grin2aa*	*grin2aa*	No F3 generation
	grin2ab				
SLC2A1	*slc2a1a*	*slc2a1a*	*slc2a1a*	*slc2a1a*	Y
	slc2a1b				
SLC6A1	*slc6a1a*	*slc6a1a*	*slc6a1a*		No Cutting
	slc6a1b	*slc6a1b*	*slc6a1b*	*slc6a1b*	Y
DNM1	*dnm1a*	*dnm1a*	*dnm1a*	*dnm1a*	No F3 generation
	dnm1b				
STXBP1	*stxbp1a*				
	*stxbp1b**				Y
SYNGAP1	*syngap1a*	*syngap1a*	*syngap1a*	*syngap1a*	No F3 generation
	syngap1b	*syngap1b*		*syngap1b*	Y
ARX	*arxa*	*arxa*	*arxa*	*arxa*	Y
	arxb				
EEF1A2	*eef1a2*	*eef1a2*	*eef1a2*	*eef1a2*	Y
HNRNPU	*hnrnpua*	*hnrnpua*	*hnrnpua*	*hnrnpua*	Y
	hnrnpub	*hnrnpub*	*hnrnpub*	*hnrnpub*	Y
MEF2C	*mef2ca*				
	mef2cb	*mef2cb*	*mef2cb*	*mef2cb*	Y
CHD2	*chd2*	*chd2*	*chd2*	*chd2*	Y
ALDH7A1	*aldh7a1*	*aldh7a1*	*aldh7a1*	*aldh7a1*	Y
PNPO	*pnpo*	*pnpo*	*pnpo*	*pnpo*	Y
CDKL5	*cdkl5*	*cdkl5*	*cdkl5*	*cdkl5*	Y
GNAO1	*gnao1a*	*gnao1a*	*gnao1a*	*gnao1a*	Y

	gnao1b	*gnao1b*	*gnao1b*	*gnao1b*	Y
TBC1D24	*tbc1d24*	*tbc1d24*	*tbc1d24*	*tbc1d24*	No F3 generation
PCDH19	*pcdh19*	*pcdh19*	*pcdh19*	*pcdh19*	Y
	pafah1b1a	*pafah1b1a*	*pafah1b1a*	*pafah1b1a*	Y
PAFAH1B1	*pafah1b1b*	*pafah1b1b*	*pafah1b1b*	*pafah1b1b*	Y
	kcna2a				
KCNA2	*kcna2b*	*kcna2b*	*kcna2b*	*kcna2b*	Y
KCNMA1	*kcnma1a*	*kcnma1a*			
	prickle1a	*prickle1a*		*prickle1a*	No F3 generation
PRICKLE1	*prickle1b*				
EPM2A	*epm2a*	*epm2a*	*epm2a*	*epm2a*	Y
SIK1	*sik1*	*sik1*	*sik1*	*sik1*	Y
	arhgef9a	*arhgef9a*	*arhgef9a*	*arhgef9a*	Y
ARHGEF9	*arhgef9b*	*arhgef9b*	*arhgef9b*	*arhgef9b*	Y
CPA6	*cpa6*	*cpa6*	*cpa6*	*cpa6*	Y
STRADA	*strada*	*strada*	*strada*	*strada*	Y
SPTAN1	*spna2*	*spna2*			
DEPDC5	*depdc5*	*depdc5*	*depdc5*	*depdc5*	Y
	cntnap2a	*cntnap2a*	*cntnap2a*	*cntnap2a*	Y
CNTNAP2	*cntnap2b*	*cntnap2b*	*cntnap2b*	*cntnap2b*	Y
	scn1ba	*scn1ba*	*scn1ba*	*scn1ba*	Y
SCN1B	*scn1bb*				
ST3GAL3	*st3gal3b*	*st3gal3b*	*st3gal3b*	*st3gal3b*	Y
PLCB1	*plcb1*	*plcb1*	*plcb1*	*plcb1*	No Cutting
GOSR2	*gosr2*	*gosr2*	*gosr2*	*gosr2*	No F3 generation
STX1B	*stx1b*	*stx1b*	*stx1b*	*stx1b*	No F3 generation
	grin1a	*grin1a*	*grin1a*	*grin1a*	Y
GRIN1	*grin1b*	*grin1b*	*grin1b*	*grin1b*	Y
Total:	**57**	**48**	**44**	**46**	

* indicate control genes with previously characterized seizure phenotypes.

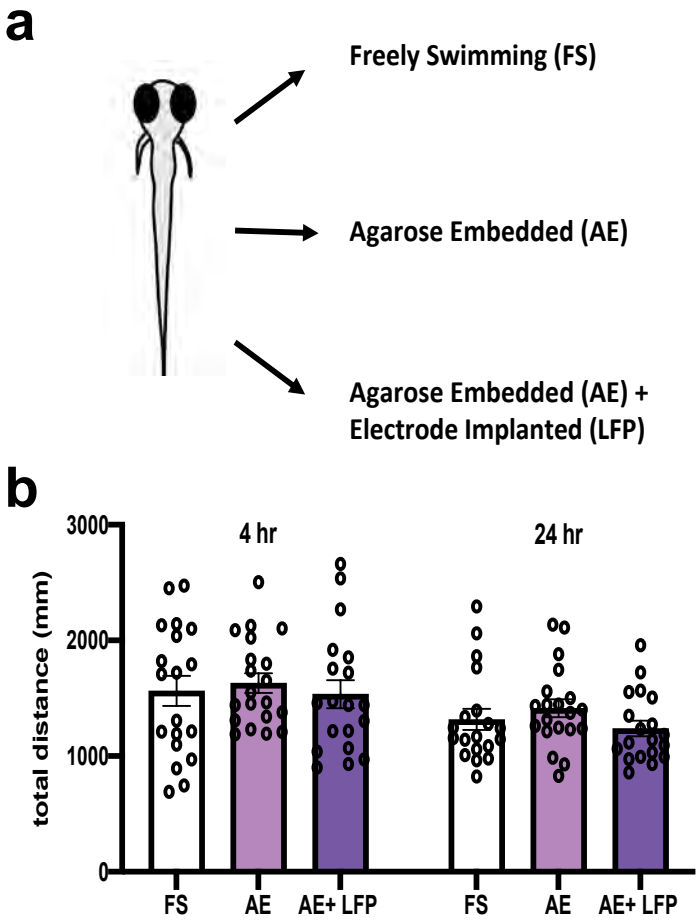
a
Freely Swimming (FS)
Agarose Embedded (AE)
Agarose Embedded (AE) +
Electrode Implanted (LFP)
b
4 hr
24 hr
total distance (mm)
3000
2000
1000
0
FS
AE
AE+ LFP
FS
AE
AE+ LFP

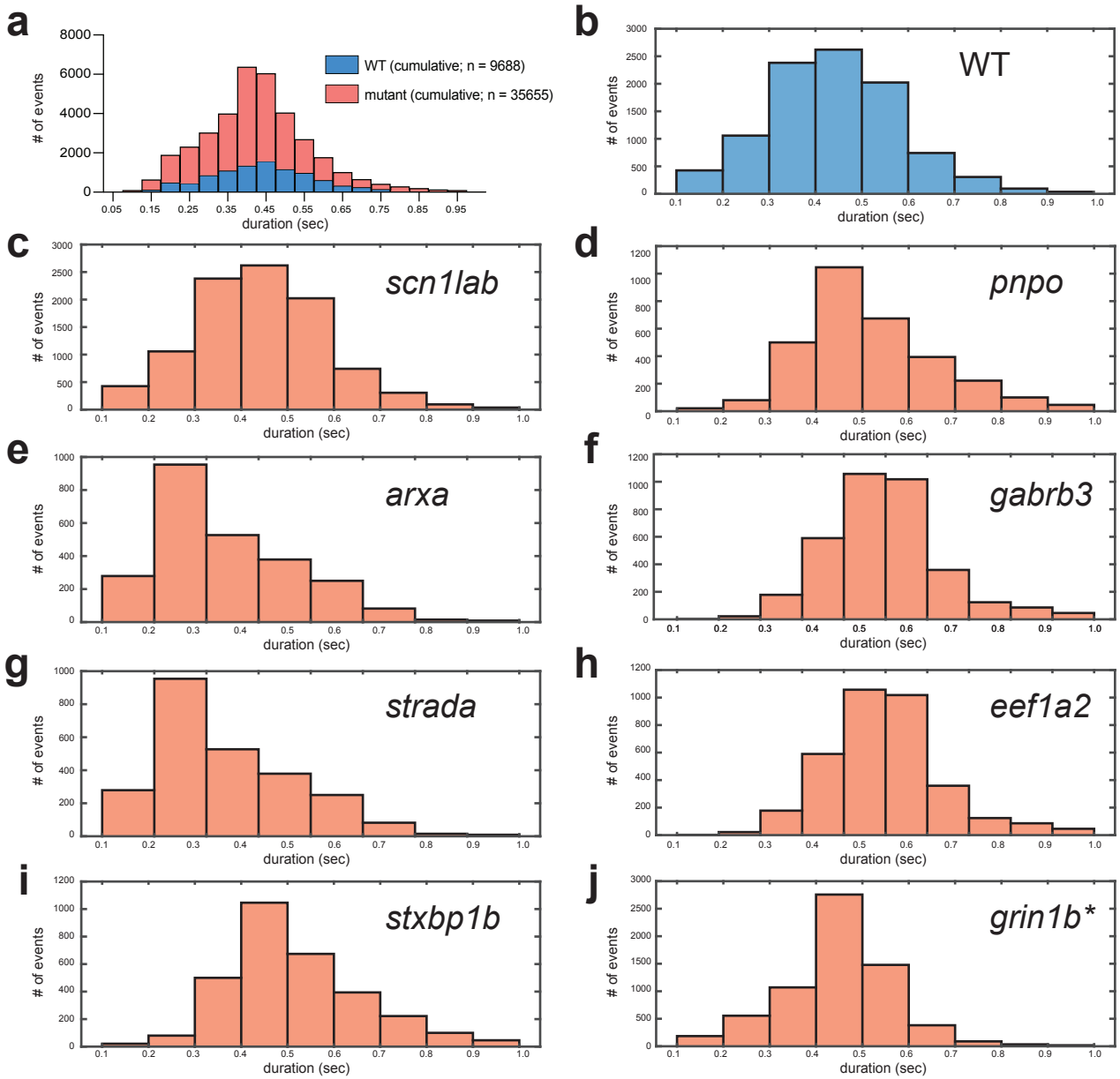
a
WT (cumulative; n = 9688)
mutant (cumulative; n = 35655)
# of events
duration (sec)
b
WT
c
scn1lab
d
pnpo
e
arxa
f
gabrb3
g
strada
h
eef1a2
i
stxbp1b
j
grin1b*

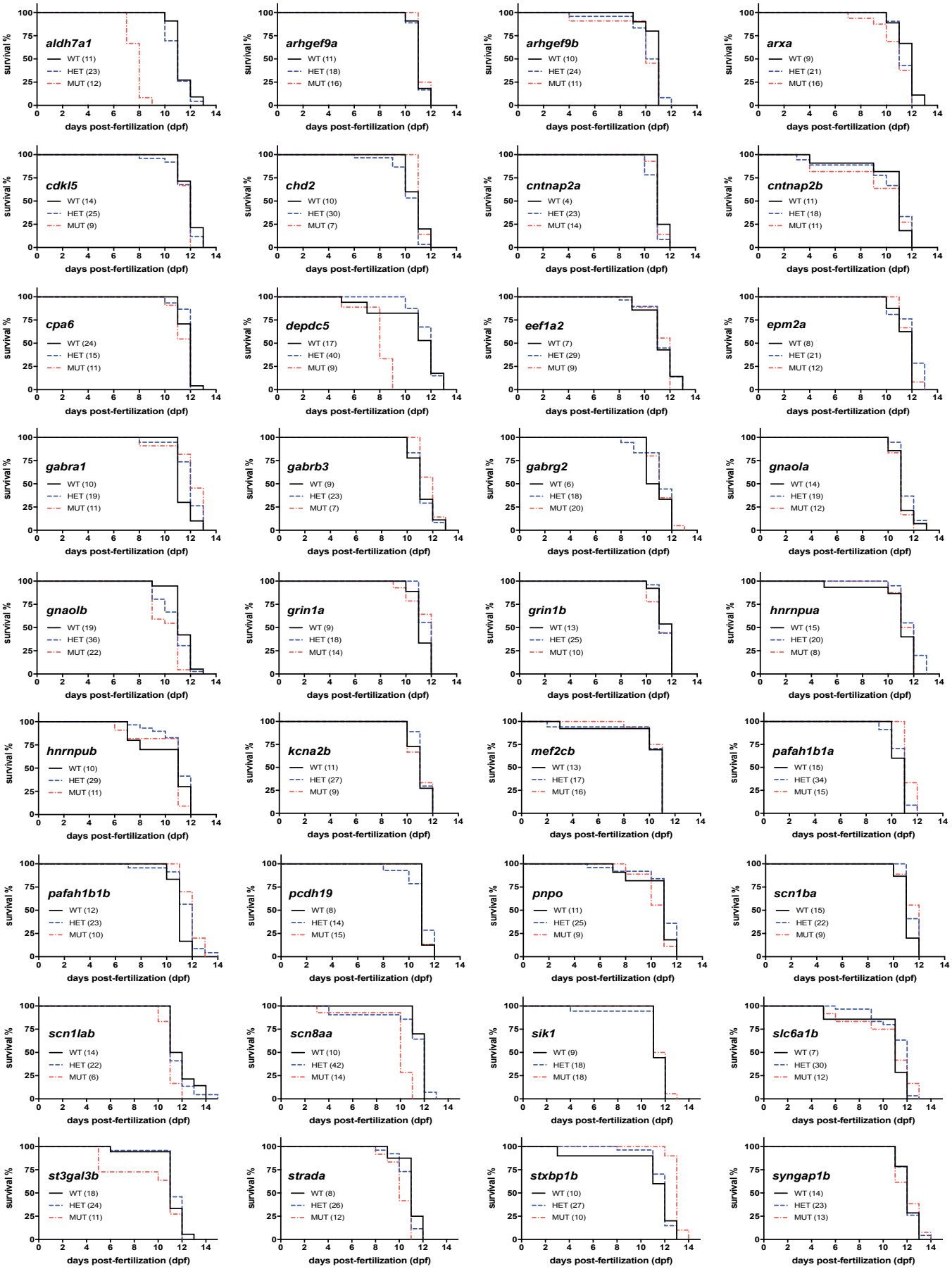
aldh7a1
WT (11)
HET (23)
MUT (12)
arhgef9a
WT (11)
HET (18)
MUT (16)
arhgef9b
WT (10)
HET (24)
MUT (11)
arxa
WT (9)
HET (21)
MUT (16)
cdkl5
WT (14)
HET (25)
MUT (9)
chd2
WT (10)
HET (30)
MUT (7)
cntnap2a
WT (4)
HET (23)
MUT (14)
cntnap2b
WT (11)
HET (18)
MUT (11)
cpa6
WT (24)
HET (15)
MUT (11)
depdc5
WT (17)
HET (40)
MUT (9)
eef1a2
WT (7)
HET (29)
MUT (9)
epm2a
WT (8)
HET (21)
MUT (12)
gabra1
WT (10)
HET (19)
MUT (11)
gabrb3
WT (9)
HET (23)
MUT (7)
gabrg2
WT (6)
HET (18)
MUT (20)
gnaola
WT (14)
HET (19)
MUT (12)
gnaolb
WT (19)
HET (36)
MUT (22)
grin1a
WT (9)
HET (18)
MUT (14)
grin1b
WT (13)
HET (25)
MUT (10)
hnrnpua
WT (15)
HET (20)
MUT (8)
hnrnpub
WT (10)
HET (29)
MUT (11)
kcna2b
WT (11)
HET (27)
MUT (9)
mef2cb
WT (13)
HET (17)
MUT (16)
pafah1b1a
WT (15)
HET (34)
MUT (15)
pafah1b1b
WT (12)
HET (23)
MUT (10)
pcdh19
WT (8)
HET (14)
MUT (15)
pnpo
WT (11)
HET (25)
MUT (9)
scn1ba
WT (15)
HET (22)
MUT (9)
scn1lab
WT (14)
HET (22)
MUT (6)
scn8aa
WT (10)
HET (42)
MUT (14)
sik1
WT (9)
HET (18)
MUT (18)
slc6a1b
WT (7)
HET (30)
MUT (12)
st3gal3b
WT (18)
HET (24)
MUT (11)
strada
WT (8)
HET (26)
MUT (12)
stxbp1b
WT (10)
HET (27)
MUT (10)
syngap1b
WT (14)
HET (23)
MUT (13)
survival %
days post-fertilization (dpf)

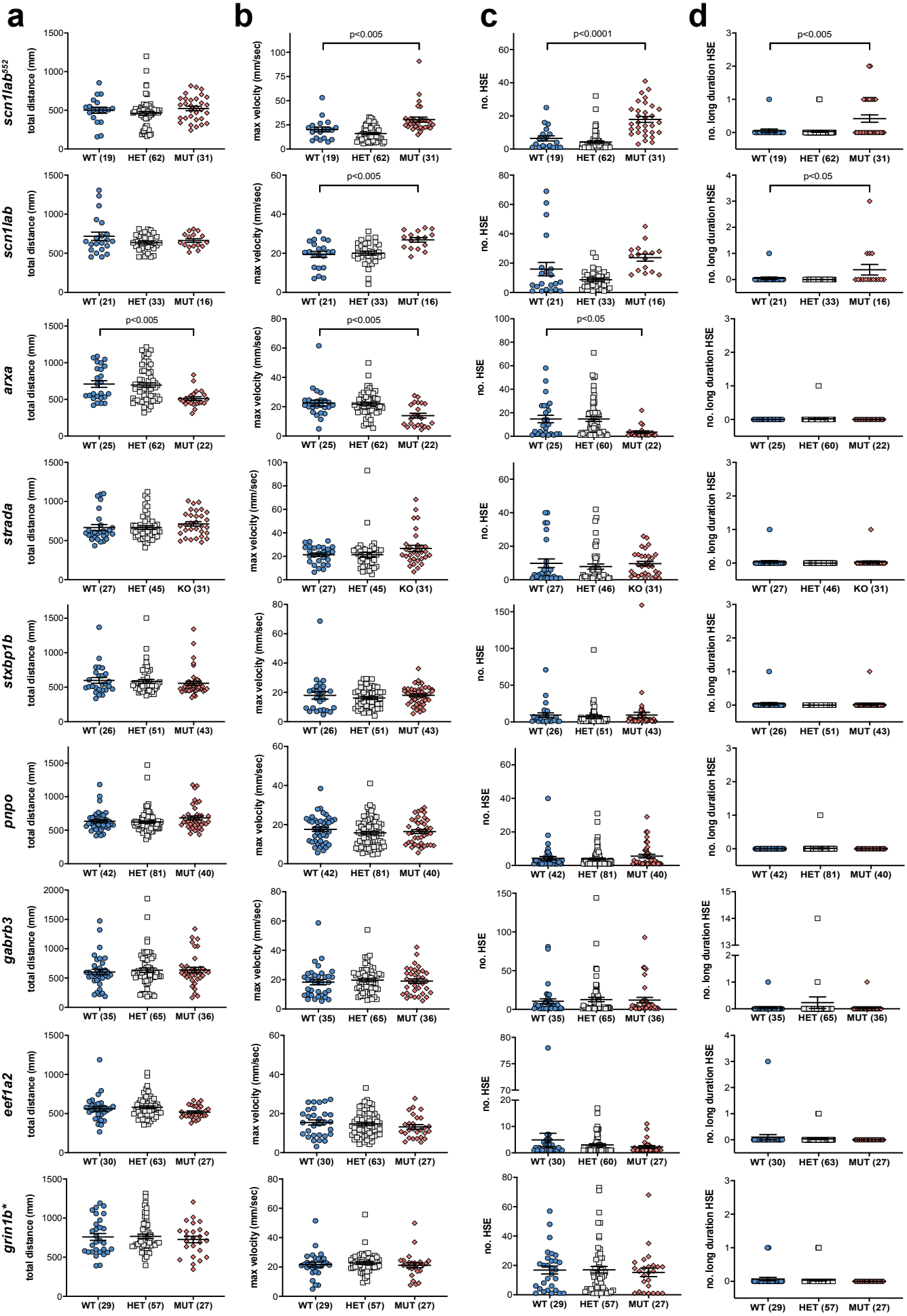
a
b
c
d
scn1lab552
scn1lab
arxa
strada
stxbp1b
pnpo
gabrb3
eef1a2
grin1b*
total distance (mm)
max velocity (mm/sec)
no. HSE
no. long duration HSE
p<0.005
p<0.0001
p<0.05
WT (19) HET (62) MUT (31)
WT (21) HET (33) MUT (16)
WT (25) HET (62) MUT (22)
WT (25) HET (60) MUT (22)
WT (27) HET (45) KO (31)
WT (27) HET (46) KO (31)
WT (26) HET (51) MUT (43)
WT (42) HET (81) MUT (40)
WT (35) HET (65) MUT (36)
WT (30) HET (63) MUT (27)
WT (30) HET (60) MUT (27)
WT (29) HET (57) MUT (27)

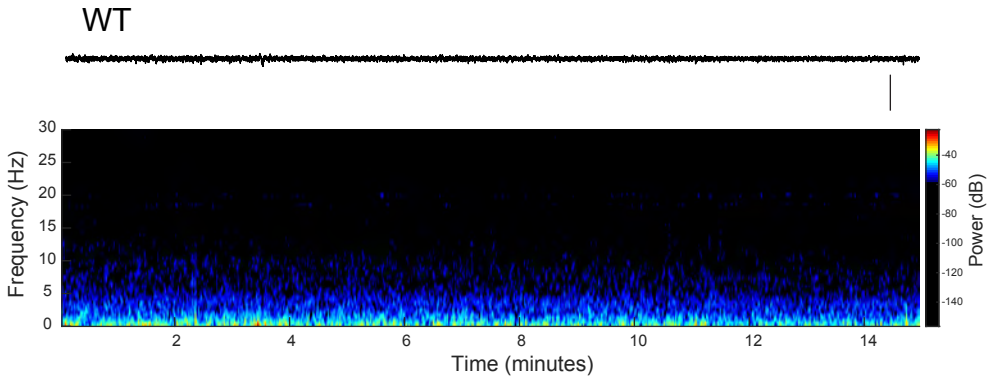
WT
Frequency (Hz)
30
25
20
15
10
5
0
2
4
6
8
10
12
14
Time (minutes)
-40
-60
-80
-100
-120
-140
Power (dB)